GIRK channel activation co-expressed with opioid receptors leads to inhibition of nociceptive transmission and thus opioid-induced analgesia [6,7,13–15].

To date, however, few studies have examined the relationship between genetic variations in GIRK channels and phenotypic differences in humans, although several studies have identified human GIRK channel gene polymorphisms [16–18]. Therefore, the present study focused on GIRK channel gene polymorphisms, particularly those of the *KCNJ6* gene encoding GIRK2 because it has been investigated more extensively than the other subtypes with regard to its involvement in analgesia [6,7,13–15]. We sought to reveal the relationship between genetic variations in the *KCNJ6* gene and individual differences in opioid analgesic sensitivity.

Methods

Ethics Statement

The study protocol was approved by the Institutional Review Boards at the Institute of Medical Science, The University of Tokyo (Tokyo, Japan), Toho University Sakura Medical Center (Sakura, Japan), and the Tokyo Institute of Psychiatry (Tokyo, Japan). All subjects provided informed, written consent for the genetics studies.

Subjects

Subjects for the resequencing of the *KCNJ6* gene were recruited from the Kanto area in Japan. A total of 48 unrelated healthy subjects were used in the study so that polymorphisms with allele frequency more than approximately 1% could be detected. The oral mucosa of the participants was collected for gene analysis.

The subjects used in the association study were 129 patients who underwent major open abdominal surgery, mostly gastrectomy for gastric cancer and colectomy for colorectal cancer, under combined general and epidural anesthesia at Research Hospital, Institute of Medical Science, The University of Tokyo, or at Toho University Sakura Medical Center. Peripheral blood or oral mucosa samples were collected from these subjects for gene analysis.

To examine *KCNJ6* gene expression levels, a total of 105 human DNA samples extracted from human occipital cortex and 100 RNA samples extracted from human anterior cingulate cortex of the same specimens were additionally obtained from the Stanley Medical Research Institute (Bethesda, MD) as samples independent of that in the association study (SMRI samples).

Clinical data

Postoperative pain was managed primarily with continuous epidural analgesia with fentanyl or morphine. Fentanyl or morphine was diluted with 0.25% bupivacaine in a total volume of 100 ml and infused at a constant rate of 2 ml/h through a catheter placed in the lower thoracic or upper lumbar epidural space. Whenever the patient complained of significant postoperative pain despite continuous epidural analgesic, appropriate doses of opioids, including morphine, buprenorphine, pentazocine, and pethidine, and/or nonsteroidal anti-inflammatory drugs (NSAIDs), including diclofenac and flurbiprofen, were administered as rescue analgesics at the discretion of surgeons. The clinical data sampled included age, gender, body height, body weight, postoperative diagnosis, type of operation, duration of operation, and doses of rescue analgesics (opioids and/or NSAIDs) administered during the first 24 h postoperative period, for which analgesic therapy would be required in most patients. The study subjects were also asked to rate their pain intensity at rest during the first 24 h postoperative period using a 5-point verbal numerical rating scale (NRS; 0 = no pain, 1 = mild pain, 2 = moderate pain, 3 = severe pain, 4 = extremely severe pain).

To allow intersubject comparisons of rescue analgesic doses required during the first 24 h postoperative period, doses of opioids and NSAIDs administered as rescue analgesics during this period were converted to the equivalent dose of oral morphine according to a previous report [19]. The conversion factor used for the different analgesics to derive equivalent doses of oral morphine is presented in Table 1. The frequency of rescue analgesic administration was determined as the frequency of use of rescue analgesics during the first 24 h postoperative period. The total dose of rescue analgesics administered was calculated as the sum of oral morphine-equivalent doses of all opioids and NSAIDs administered to patients as rescue analgesics during the same period.

Resequencing KCNJ6 and SNP selection for the association study

To comprehensively screen polymorphisms in the *KCNJ6* gene, resequencing was performed using an ABI PRISM® 3100 Genetic Analyzer (Life Technologies Japan Ltd., Tokyo, Japan) for the human *KCNJ6* (*GIRK2*) gene regions (mapped to 21q22.13–q22.2) and 5′-flanking region based on the nucleotide sequences of the GenBank database (accession number: NT_011512). The screened regions contained all consensus sequences of exon regions, exon-intron boundary regions (approximately 30 bp), and putative promoter regions (approximately 1.8 kbp) for the gene. The total length of the screened regions approximately amounted to 4.5 kbp (Figure 1). All primers used for the screening are shown in Table 2.

Single-nucleotide polymorphisms (SNPs) for the association studies were selected based on several factors, including recently advanced tagging strategies [20–22]. To identify relationships between the SNPs identified in the polymorphism screening, linkage disequilibrium (LD) analysis was performed using Haploview v. 3.32 [23]. For estimation of LD strength between the SNPs, the commonly used D' and r^2 values were pairwise calculated using the genotype dataset of each SNP. LD blocks were defined among the SNPs showing "strong LD," based on the default algorithm of Gabriel et al. [24], in which the upper and lower 95% confidence limits on D' for strong LD were set at 0.98 and 0.7, respectively. Tag SNPs in the LD block were consequently determined by the software package Tagger, which is incorporated in Haploview and has been detailed in a previous report [22].

Table 1. Estimated systemic dose equipotent to 90 mg oral morphine (mg).

Analgesics	Dose	Reference
Morphine (oral)	90	[39]
Morphine (intravenous)	30	[39]
Morphine (epidural)	6	[39,40]
Pentazocine	90	[39,41]
Buprenophine	1	[39,41]
Petidine	360	[39,42]
Fentanyl	0.3	[39,43]
Diclofenac	300	[39,43–45]
Flurbiprofen	300	[39,43–47]
Indomethacin	300	[39,43–47]

doi:10.1371/journal.pone.0007060.t001

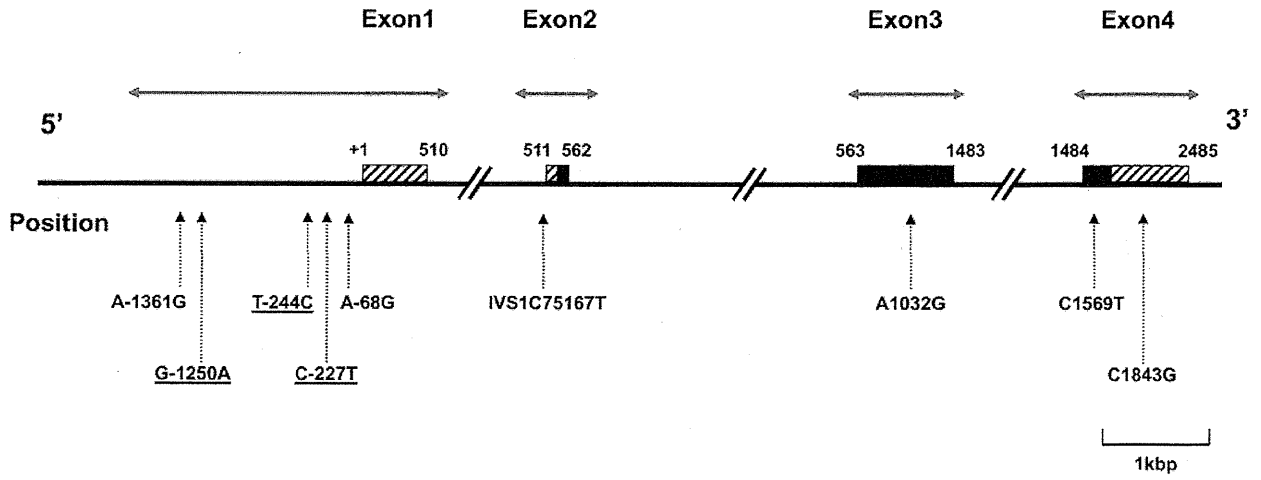

Figure 1. The position of the SNPs identified in the polymorphism screening for the *KCNJ6* gene. The filled box and striped box represent the coding region and untranslated region, respectively. The horizontal arrows indicate the screened regions. The numbers above the boxes and in the exonic SNPs are relative positions from the transcription start site (+1) in the *KCNJ6* mRNA, and the number "75167" in the IVS1C75167T SNP is the relative position from the intron 1 start site in the genomic DNA. The underlined SNPs show absolute linkage disequilibrium between one another ($D'=1$, $r^2=1$).
doi:10.1371/journal.pone.0007060.g001

Genotyping

Total genomic DNA was extracted from peripheral blood or oral mucosa samples by standard procedures.

For genotyping *KCNJ6* G-1250A, the polymerase chain reaction-restriction fragment length polymorphism (PCR-RFLP) method and direct sequencing were adopted. To perform PCR-RFLP, the restriction enzyme BsmI (Toyobo Co., Ltd., Tokyo, Japan) and two primers of P5F and P6R were used (Table 2). First, PCR was performed in a final volume of 10 µl containing 5×GoTaq™ reaction buffer (7.5 mM magnesium), 0.16 mM dioxyribonucleoside triphosphate (dNTP), 0.4 µM of each primer, 0.5 U GoTaq™ DNA polymerase (Promega K.K. Japan, Tokyo, Japan), and 5–50 ng extracted genomic DNA as the template. The PCR program was the following: 95°C for 2 min, followed by 35 cycles of 95°C for 30 s, 60°C for 30 s, and 72°C for 1 min, with a final extension at 72°C for 8 min. The amplified DNA fragments were digested by the restriction enzyme at 65°C in a total of 15 µl reaction solution containing 10×M buffer (100 mM Tris-HCl, pH 7.5, 100 mM $MgCl_2$, 500 mM NaCl, 10 mM dithiothreitol), 0.3 U BsmI, and 3.5 µl PCR product as the substrate. The digestion products were analyzed by electrophoresis using 1–2% agarose gel and ethidium bromide staining for visualization under ultraviolet illumination. The appearance of only the 601 bp DNA fragment corresponded to the A/A genotype of the loaded sample. The appearance of both the 233 bp and 370 bp fragments corresponded to the G/G genotype, and the appearance of all three 601 bp, 233 bp, and 370 bp DNA fragments corresponded to the G/A genotype. The failure rate of the RFLP genotyping assays was 1.667%.

For genotyping *KCNJ6* A1032G, the PCR-RFLP method, TaqMan allelic discrimination assay (Life Technologies Japan Ltd.) and direct sequencing were adopted. To perform PCR-RFLP, the restriction enzyme BspEI (New England Biolabs, Inc., Ipswich, MA) was used. The forward primer P23F and the reverse primer P24R were used (Table 2). First, PCR was performed in a final volume of 10 µl containing 5×GoTaq™ reaction buffer (7.5 mM magnesium), 0.16 mM dNTP, 0.4 µM of each primer, 0.5 U GoTaq™ DNA polymerase (Promega K.K. Japan, Tokyo, Japan), and 5–50 ng extracted genomic DNA as the template. The PCR program was the following: 95°C for 2 min, followed by 35–40 cycles of 95°C for 30 s, 50°C for 30 s, and 72°C for 1 min, with a final extension at 72°C for 8 min. The amplified DNA fragments were digested by the restriction enzyme at 37°C in a total of 10 µl reaction solution containing 10×NEBuffer 3 (500 mM Tris-HCl, pH 7.9, 100 mM $MgCl_2$, 1000 mM NaCl, 10 mM dithiothreitol), 0.5 U BspEI, and 5 µl PCR product as the substrate. The digestion products were analyzed by electrophoresis using 1–2% agarose gel and ethidium bromide staining for visualization under ultraviolet illumination. A 65 bp digested DNA fragment is not easily distinguishable; therefore, the appearance of 395 bp, 332 bp, and both 395 bp and 332 bp DNA fragments corresponded to the A/A, G/G, and A/G genotypes, respectively, of the loaded sample. The failure rate of the RFLP genotyping assays was 3.571%. To perform the TaqMan allelic discrimination assay with a LightCycler 480 (Roche Diagnostics K.K., Tokyo, Japan), TaqMan® SNP Genotyping Assays (Life Technologies Japan Ltd.) containing sequence-specific forward and reverse primers to amplify the polymorphic sequence and two probes labeled with VIC® and FAM™ dye to detect both alleles of the *KCNJ6* A1032G (Assay ID: C_15868122_10) were used. Real-time PCR was performed in a final volume of 10 µl containing 2×LightCycler® 480 Probes Master (Roche Diagnostics K.K.), 40×TaqMan® Gene Expression Assays, 5 ng genomic DNA as the template, and up to 10 µl H_2O equipped with 2×LightCycler® 480 Probes Master. The thermal condition was the following: 95°C for 10 min, followed by 45 cycles of 95°C for 10 s and 60°C for 60 s, with a final cooling at 50°C for 30 s. Afterward, endpoint fluorescence was measured for each sample well, and the A/A, A/G, and G/G genotypes were determined based on the presence or absence of each type of fluorescence.

For samples that were difficult to genotype for *KCNJ6* G-1250A and *KCNJ6* A1032G using the PCR-RFLP method, direct sequencing was adopted to determine the sequence with both forward and reverse primers enclosing the SNP sites.

Real-time quantitative PCR (qPCR)

The SMRI RNA samples were treated with DNase I using RNase-Free DNase Set (QIAGEN K.K., Tokyo, Japan) at room temperature (20–25°C) for 10 min, and then clean-up was performed using RNeasy® MinElute® Cleanup Kit (QIAGEN).

Table 2. Primers used in the analyses.

Gene	Region	Sequence	Forward/Reverse	Primer No.
KCNJ6	5′-flanking	TCCCAGTTGCAGTGGACAGGAC	Forward	P1F
		AAATCCCCGGTTAGGAGAAAAGTG	Reverse	P2R
		CCAGTTATTGAAAGGGCCATTATA	Forward	P3F
		CTAAGTAAGTTATTCCCGGAGAAA	Reverse	P4R
		CAGGCATTGTGGAGCACGTATTAC	Forward	P5F
		CACCCCCTCTTTTTCTTATGGTCA	Reverse	P6R
		AATGGGATCCATCTCATTCAACAC	Forward	P7F
		AGAAGGCTTACGGAAACCTCTTAT	Reverse	P8R
	Exon 1	CGGCGGGGTGGGCGTCTC	Forward	P9F
		CCCCCGTGCGAGTTTCAGTCG	Reverse	P10R
		TCGCCCCCGCCCCTTCCT	Forward	P11F
		TCCCTCGCCTTTCGGCTGACTTG	Reverse	P12R
	Exon 2	TTTTGAAAACTGGTCGTGCGTCAC	Forward	P13F
		TTCTGTCTGAAATTTCTGAACG	Reverse	P14R
	Exon 3	AAGTCAACTAGAGGCCTATCCAGA	Forward	P15F
		CTAAGGTCCCCTACCCGGAACATC	Reverse	P16R
		CTGGTGGGCAGGATGGTGAA	Forward	P17F
		TCTCTGCCCTCTTCTTGGGTTGAG	Reverse	P18R
		TTGATCGCATACATACGGGGAGAC	Forward	P19F
		GTCATGAAGCAAGGGGATGTTGTC	Reverse	P20R
		TGGCTACCGGGTCATCACAGATAA	Forward	P21F
		GGCTTCTTGGTGGATATACTTCAG	Reverse	P22R
		TTCTCAATAGAGACAGAAACCACCATTGGT-	Forward	P23F
		TATGGCTACCGGGTCATCACAGATAAATGT		
		GACACCAGAAACAGACGGTCATC	Reverse	P24R
		GGATGAACTCCCCCTCCGAGGTCT	Reverse	P25R
	Exon 4	ACCTACTAAGTGTGGCATCGTATG	Forward	P26F
		AACACATGCAGGTAAGTAACTGAA	Reverse	P27R
		CCCTAGCTGGGCAAACCCTTCTC	Forward	P28F
		TTCCCCCAGACCTATGGCTTGTTG	Reverse	P29R
		TGTGGCAAACCTGGAGAATGAATC	Forward	P30F
		GATCCGTGTGGGAACAGTGAGGTA	Reverse	P31R

Forward/Reverse, sense/antisense strand sequences of the gene, respectively; Primer No., the ID number of the primer described in the paper.
doi:10.1371/journal.pone.0007060.t002

First-strand cDNA for use in real-time qPCR was synthesized with the SuperScriptIII First-Strand synthesis system for qRT-PCR (Life Technologies Japan Ltd.) with 100 ng purified total RNA according to the manufacturer's protocol.

To perform real-time qPCR utilizing a LightCycler 480 (Roche Diagnostics K.K.), TaqMan® Gene Expression Assays (Life Technologies Japan Ltd.) were used as a probe/primer set specified for the *KCNJ6* gene (Assay ID: Hs01040524_m1) and a probe/primer set for the *ACTB* gene, a house-keeping gene, encoding β-actin (Assay ID: Hs99999903_m1). PCR was performed in a final volume of 20 µl containing 2×LightCycler® 480 Probes Master, 1 µl TaqMan® Gene Expression Assay, 1 µl cDNA as the template, and up to 20 µl H_2O equipped with 2×LightCycler® 480 Probes Master. The PCR program was the following: 95°C for 10 min, 45 cycles of 95°C for 10 s and 60°C for 30 s, followed by 95°C for 10 s, 50°C for 30 s, 50–70°C (continuously) at a rate 0.06°C/s, with a final cooling at 50°C for 30 s. The expression level of the *KCNJ6* gene was normalized to that of the *ACTB* gene for each sample, and relative *KCNJ6* mRNA expression levels between all samples were compared by setting the lowest expression level among all SMRI samples as 1. Experiments were performed in duplicate (separate experiments) for each sample, and averaged values were calculated for normalized expression levels.

Predictions of mRNA secondary structure

To discuss in depth mRNA sequence and function, the secondary structure for *KCNJ6* mRNA was predicted using Mfold web server (v. 3.2) with default settings [25]. The *KCNJ6* mRNA position 982–1082 was used to predict the local structure of the mRNA based on the nucleotide sequences of the GenBank database (accession number: NM_002240.2).

Statistical analysis

The χ^2 test or Fisher exact test was performed for all genotype frequency data using FreeJSTAT 8.2 for Windows (free software by

Table 3. The characteristics of the identified SNPs in the *KCNJ6* gene.

Position	SNP name	rs ID	Sample size	Reported allele	Major allele	Minor allele	Minor allele frequency
5′-flanking	A-1361G	–	48	A	A	G	0.010 (N.A.)
	G-1250A	rs6517442	48	G	A	G	0.385 (0.422)
	T-244C	rs7275707	46	T	C	T	0.391 (0.422)
	C-227T	rs7276069	46	C	T	C	0.391 (0.422)
	A-68G	rs11702683	45	A	G	A	0.089 (0.102)
Intron 1	IVS1C75167T	rs2836016	48	C	T	C	0.188 (0.273)
Exon 3	A1032G	rs2070995	48	A	G	A	0.344 (0.432)
Exon 4	C1569T	rs702859	48	C	T	C	0.062 (0.100)
	C1843G	rs56345212	48	C	C	G	0.052 (N.A.)

rs ID, reference SNP ID in the NCBI dbSNP database; Sample size, the number of samples used for genotyping each SNP; Reported allele, the allele appearing in the GenBank reference sequence. The numbers in parentheses represent the minor allele frequencies for the Japanese population described in the NCBI dbSNP database. N.A., not available.

doi:10.1371/journal.pone.0007060.t003

M. Sato, Japan; current version is available at http://www.vector.co.jp/soft/win95/business/se030917.html) or Simple Interactive Statistical Analysis (free software by Quantitative Skills, The Netherlands; current version is available at http://www.quantitativeskills.com/sisa/) to investigate the deviation of the distributions from those in the theoretical Hardy-Weinberg equilibrium. Analysis of covariance (ANCOVA) was performed to examine the contribution of the SNPs to the subjective pain ratings reported by patients, frequency of 24 h analgesic requirements, and analgesic requirements during the 24 h postoperative period. Bonferroni multiple comparisons were used as *post hoc* tests. Correction of multiple testing was not performed for the results of the G-1250A and A1032G SNPs in this explorative study. The age, height, and weight of the subjects were incorporated as covariables for the ANCOVA because these three factors were found to be significant covariables in a preliminary analysis and may affect analgesic efficacy of opioids and/or NSAIDs. Pearson's correlation coefficient (r) was calculated to examine the correlation between variables. Student's t-test was performed to compare *KCNJ6* expression levels between the A1032G genotype subgroups. For these three analyses, SPSS 12.0J for Windows (SPSS Japan, Inc., Tokyo, Japan) was used. Power analyses were performed using G*Power Version 3.0.5 [26]. gPLINK v. 2.049, PLINK v. 1.01 (http://pngu.mgh.harvard.edu/purcell/plink/) [27], and Haploview v. 4.0 [23] were used for haplotype-specific tests, incorporating gender, age, height, and weight of the subjects as covariables, with the false discovery rate set at 0.05 for correction of multiple testing, based on a previous report [28]. In all statistical tests, the criterion for significance was set at $P<0.05$.

Results

In the first polymorphism search in the whole exon, 5′-flanking, and exon-intron boundary regions of the *KCNJ6* gene, a total of nine SNPs were identified in the 5′-flanking region, intron 1, exon 3, and exon 4. Figure 1 illustrates the relative positions of the SNPs identified in the *KCNJ6* gene. The characteristics of the SNPs are provided in Table 3, where the minor allele frequencies of the SNPs are also shown. The allele frequencies of the SNPs observed in this study were comparable (less than 0.1 difference) to those annotated in the National Center for Biotechnology Information (NCBI) database (Table 3). SNPs for a further association study were selected, considering the LD structure, minor allele frequencies of the SNPs, and the expected impact on gene function. The results of the D' and r^2 calculations for the *KCNJ6* gene are provided in Table 4. Absolute LD ($D'=1$, $r^2=1$) was observed between SNPs G-1250A, T-244C, and C-227T (Table 4),

Table 4. Pairwise D' and r^2 values between the identified SNPs in the *KCNJ6* gene.

		D'							
	SNP name	A-1361G	G-1250A	T-244C	C-227T	A-68G	IVS1C75167T	A1032G	C1569T	C1843G
	A-1361G	–	1.000	1.000	1.000	1.000	1.000	1.000	1.000	1.000
	G-1250A	0.017	–	***1.000***	***1.000***	1.000	0.136	0.037	0.518	0.159
	T-244C	0.017	***1.000***	–	***1.000***	1.000	0.114	0.020	0.505	0.104
r^2	C-227T	0.017	***1.000***	***1.000***	–	1.000	0.114	0.020	0.505	0.104
	A-68G	0.000	0.153	0.153	0.153	–	0.191	0.398	0.152	0.093
	IVS1C75167T	0.002	0.007	0.005	0.005	0.014	–	0.078	1.000	0.044
	A1032G	0.020	0.000	0.000	0.000	0.034	0.003	–	0.603	0.401
	C1569T	0.001	0.029	0.028	0.028	0.000	0.015	0.046	–	0.091
	C1843G	0.192	0.002	0.001	0.001	0.004	0.000	0.017	0.007	–

The numbers above and below the hyphens show the results of the pairwise calculations of D' and r^2 between the two SNPs, respectively. The values representing $D'=1.000$ are underlined. The pairs of values representing $D'=1.000$ and $r^2=1.000$ are italicized and bold.

doi:10.1371/journal.pone.0007060.t004

and Haploview also identified G-1250A as a candidate haplotype-tagging SNP in this LD block structure. The minor allele frequencies for these three SNPs were relatively high (Table 3), and G-1250A was selected for the association study. Among the remaining six SNPs, IVS1C75467T and A1032G are relatively common, with minor allele frequencies greater than 0.1, and could be candidates for an association study. Because IVS1C75467T is in the intron region and thus is less likely to affect the mRNA product or protein levels, it was not selected as a candidate SNP. Therefore, G-1250A and A1032G were selected from the nine *KCNJ6* SNPs for the association study.

The genotype distributions for the two SNPs that were selected were not significantly different from the theoretical Hardy-Weinberg equilibrium values in independent tests of the 48 healthy subjects used in the resequencing procedure or 129 patient subjects used in the association analyses (data not shown). The clinical data of the 129 subjects who were included in the association study are provided in Table 5. Rescue analgesics were required in 59 patients. Doses of rescue analgesics administered to patients are shown in Table 5. More detailed clinical data stratified by each genotype (*KCNJ6* G-1250A and A1032G) are presented as Supporting Information in Table S1.

Two-way ANCOVA was performed to examine the effects of SNPs and gender on the frequency of rescue analgesic administration, the total dose of rescue analgesics administered, and NRS pain scores, incorporating the age, height, and weight of the subjects as covariables. Statistical power analyses for the ANCOVA revealed that the expected power (1 minus type II error probability) was 71% for the Cohen's conventional "medium" effect size 0.25 [29] when the sample size was 129 and type I error probability was set at 0.05. Significant associations were not observed between *KCNJ6* G-1250A and the frequency of rescue analgesic administration or total dose of rescue analgesics administered (frequency of rescue analgesic administration: $F_{2,117} = 1.145$, $P = 0.322$; total dose of rescue analgesics administered: $F_{2,117} = 1.233$, $P = 0.295$). A significant main effect of *KCNJ6* A1032G on the frequency of rescue analgesic administration was observed ($F_{2,120} = 5.336$, $P = 0.006$). *Post hoc* analysis revealed significant differences between the A/A and A/G genotypes ($P = 0.005$) and between the A/A and G/G genotypes ($P = 0.010$), indicating that the carriers of the A/A genotype in the A1032G SNP required rescue analgesics more often compared with carriers of the A/G and G/G genotypes (Figure 2A). The effect of *KCNJ6* A1032G on the total dose of rescue analgesics administered was not significant ($F_{2,120} = 1.332$, $P = 0.268$). However, a significant main effect of the *KCNJ6* A1032G SNP on the total dose of rescue analgesics administered was observed in the female subjects ($F_{2,49} = 3.428$, $P = 0.040$), and differences were

Table 5. The clinical data of the subjects included in the study.

	N	Minimum	Maximum	Mean	SD
***KCNJ6* G-1250A**					
G/G (male/female)	19 (11/8)				
G/A (male/female)	72 (42/30)				
A/A (male/female)	35 (19/16)				
***KCNJ6* A1032G**					
A/A (male/female)	11 (5/6)				
A/G (male/female)	62 (37/25)				
G/G (male/female)	56 (32/24)				
Gender					
male	74				
female	55				
Age	129	28	80	63.57	9.92
Height (cm)	129	133	175	158.21	8.34
Weight (kg)	129	35	80	56.24	10.42
NRS pain score	105	0	4	1.54	1.29
male/female	62/43	0/0	4/4	1.48/1.63	1.21/1.40
Frequency of analgesic administration	129	0	6	0.72	1.01
male/female	74/55	0/0	3/6	0.70/0.75	0.90/1.14
Total dose of rescue analgesics (mg)	129	0	105	12.63	19.16
male/female	74/55	0/0	72/105	13.38/11.62	19.05/19.44
Dose of each rescue analgesic (mg)	129	(0)	(105)	(12.63)	(19.16)
Epidural morphine (mg)	2	0.5 (7.5)	2 (30)	1.25 (18.75)	1.06 (15.91)
Pentazocine (mg)	24	15 (15)	75 (75)	26.25 (26.25)	17.83 (17.83)
Buprenophine (mg)	15	0.2 (18)	0.8 (72)	0.47 (42.00)	0.16 (14.70)
Petidine (mg)	1	35 (8.75)	35 (8.75)	35.00 (8.75)	–
Diclofenac (mg)	14	25 (7.5)	100 (30)	37.50 (11.25)	23.51 (7.054)
Flurbiprofen (mg)	8	50 (15)	100 (30)	62.50 (18.75)	23.15 (6.944)

Values in parentheses for "Dose of each rescue analgesic (mg)" indicate data for dose of each rescue analgesic converted to the equivalent oral morphine dose.

doi:10.1371/journal.pone.0007060.t005

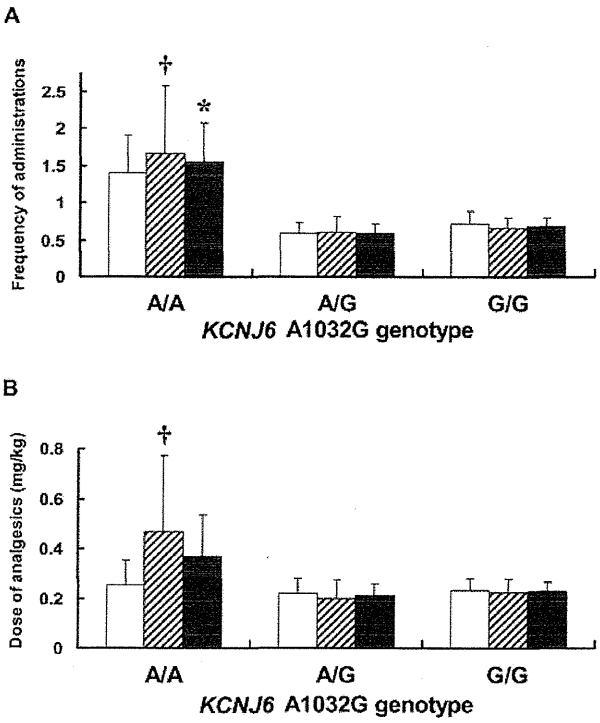

Figure 2. Association analysis between requirements for rescue analgesics and SNPs. The results for the frequency of analgesic administration (A) and the total dose of analgesics administered per weight (B) during the 24 h postoperative period are shown for the *KCNJ6* A1032G SNP. The white, striped, and filled boxes indicate results for male, female, and all subjects, respectively. (A) *: significantly more frequent administration for the A/A genotype compared with the A/G and G/G genotypes in all subjects, †: significantly more frequent administration for the A/A genotype compared with the A/G and G/G genotypes in female subjects. (B) †: significantly greater dose of analgesic administration for the A/A genotype compared with the A/G genotype in female subjects.
doi:10.1371/journal.pone.0007060.g002

significant between the A/A and A/G genotypes ($P = 0.040$) and marginally significant between the A/A and G/G genotypes ($P = 0.061$) in the *post hoc* analysis (Figure 2B), whereas such differences were not observed in male subjects ($F_{2,68} = 0.032$, $P = 0.969$). Neither the main effect of gender nor the SNP×gender interaction was significant (data not shown). Significant associations were not observed between the two SNPs and NRS pain scores (G-1250A: $F_{2,94} = 1.455$, $P = 0.239$; A1032G: $F_{2,96} = 0.115$, $P = 0.892$), although significant positive correlations were found between NRS pain scores and frequency of rescue analgesic administration ($r = 0.281$, $P = 0.004$) and between NRS pain scores and total dose of rescue analgesics administered ($r = 0.266$, $P = 0.006$), indicating that the patients who received analgesics more frequently felt more pain, possibly attributable to insufficient analgesic effects.

To examine in more detail the association between *KCNJ6* SNPs and rescue analgesic requirements, a haplotype-based test was performed. As shown in Table 6A, a significant association was found between the −1250G/1032A haplotype and the increased frequency of rescue analgesic administration in all patient subjects ($R^2 = 0.120$, adjusted $P = 0.015$). Although no significant associations were observed between each of the *KCNJ6* haplotypes and total dose of rescue analgesics administered in all patient subjects and male subjects ($R^2 = 0.080$, $P = 0.328$; $R^2 = 0.028$, $P = 0.765$, respectively), the −1250G/1032A haplotype was significantly associated with total dose of rescue analgesics administered in female subjects ($R^2 = 0.277$, adjusted $P = 0.038$; Table 6B). Associations between each of the G-1250A/A1032G haplotypes and NRS pain scores were not significant (data not shown).

To estimate the impact of the *KCNJ6* A1032G polymorphism on gene expression level, the relative *KCNJ6* mRNA expression level was compared between the genotype subgroups of the SMRI samples in the real-time qPCR. The relative expression level (mean±SEM) was 1.59±0.17, 2.07±0.08, and 1.99±0.06 for the A/A, A/G, and G/G genotypes in the A1032G SNP, respectively (Figure 3), demonstrating that the expression level was 0.76–0.80 fold lower in the A/A genotype than in the A/G and G/G genotype. The difference was significant between the A/A genotype and combined A/G and G/G genotypes ($t_{98} = 2.265$, $P = 0.026$).

Table 6. Association of *KCNJ6* haplotypes with postoperative analgesia.

A						
Haplotype	**Frequency**	**Beta**	**R^2**	**F**	***P***	***P**^a^*
−1250G/1032A	0.1517	0.6313	0.1197	8.8080	0.0036†	0.0145*
−1250A/1032A	0.1736	−0.0216	0.0546	0.0101	0.9203	0.9203
−1250G/1032G	0.2848	−0.0754	0.0563	0.2211	0.6391	0.8521
−1250A/1032G	0.3898	−0.2179	0.0711	2.1290	0.1472	0.2944
B						
Haplotype	**Frequency**	**Beta**	**R^2**	**F**	***P***	***P**^a^*
−1250G/1032A	0.1394	0.3139	0.2771	7.3160	0.0094†	0.0377*
−1250A/1032A	0.2032	−0.0160	0.1673	0.0192	0.8903	1.0000
−1250G/1032G	0.2865	−0.0273	0.1687	0.0995	0.7538	1.0000
−1250A/1032G	0.3709	−0.1054	0.1951	1.6770	0.2015	0.8903

Association of the haplotype composed of the G-1250A/A1032G SNPs with (A) the frequency of analgesic administration in all patient subjects or (B) the total dose of analgesics administered during the 24 h postoperative period in female patient subjects. Frequency, haplotype frequency; Beta, regression coefficient; R^2, coefficient of determination; F, *F* statistic; *P*, crude *P* value; P^a, adjusted *P* value for multiple testing. †$P<0.05$, *$P^a<0.05$.
doi:10.1371/journal.pone.0007060.t006

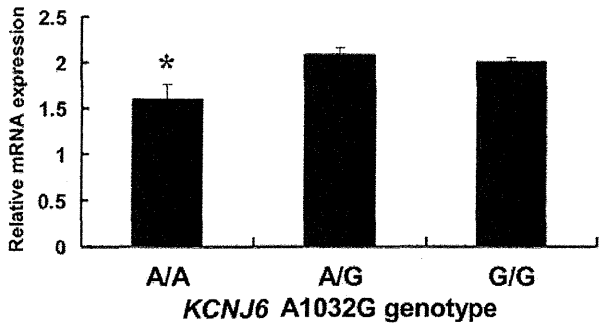

Figure 3. Relative *KCNJ6* mRNA expression level between each genotype subgroup of the SMRI samples. *: significantly lower expression level between the A/A genotype and combined A/G and G/G genotypes in all subjects.
doi:10.1371/journal.pone.0007060.g003

Discussion

The present study comprehensively examined *KCNJ6* genetic variations in humans and explored the associations between these variations and outcomes in clinical pain management. To our knowledge, the present study is the first to explore SNPs of the *KCNJ6* gene with regard to associations between these SNPs and postoperative analgesic requirements in humans. We found that carriers of the A/A genotype in the A1032G SNP or −1250G/1032A haplotype required rescue analgesics more often and tended to require higher doses of rescue analgesics, especially in female subjects, compared with carriers of other genotypes or haplotypes, respectively, after major open abdominal surgery (Figure 2A and B, Table 6). Although we did not show all of the results of multiple testing for the G-1250A and A1032G SNPs with the Bonferroni correction because this study was explorative, the *P* value for the main effect of *KCNJ6* A1032G on the frequency of rescue analgesic administration was 0.012 after the Bonferroni correction. This suggests that this SNP is likely to affect sensitivity to analgesics, although we must concede that this significance might possibly occur by chance alone. Patients who experienced more severe pain, evaluated by NRS pain scores, required higher-dose and more frequent rescue analgesics, although significant associations were not observed between the A1032G SNP or −1250G/1032A haplotype and NRS pain scores. Moreover, *KCNJ6* gene expression levels in the 1032A/A subjects was significantly decreased compared with 1032A/G and 1032G/G subjects in the real-time qPCR analysis using human brain tissues, suggesting that the 1032A/A subjects required more analgesics because of lower *KCNJ6* gene expression levels and consequently insufficient analgesic effects. Altogether, these results suggest that subjects carrying the A/A genotype in the A1032G SNP or −1250G/1032A haplotype, especially in females, had lower sensitivity to analgesics and, therefore, required more rescue analgesics than subjects carrying other genotypes or haplotypes to achieve a similar degree of pain relief.

For our ANCOVA analyses, the desirable sample size was calculated as 158 for the effect size 0.25 to achieve 80% power. This might suggest that a sample size of 129 subjects in our study was somewhat insufficient to reliably detect moderate differences between the SNP genotypes, and a far greater sample may be required to detect smaller differences. Considering this caveat and relatively small effect size observed in the haplotype analysis (e.g., R^2 for haplotype effect on the frequency of analgesic administration was 0.120), future studies with larger sample sizes may reveal additional associations between polymorphisms and opioid sensitivity.

In the initial polymorphism screening for *KCNJ6*, a total of nine SNPs were identified in the whole exon, 5′-flanking, and exon-intron boundary regions (Figure 1). Polymorphisms that might cause significant functional changes, such as nonsynonymous or insertion/deletion polymorphisms, were not found in the polymorphism screening of the human *KCNJ6* gene in the present study, possibly attributable to the importance and high conservation of mammalian GIRK channels. A possible explanation derives from studies in *weaver* mice, in which only a single missense mutation in the pore region of the mouse *Kcnj6* gene causes various aberrant changes in cerebellar granule cells [30], membrane permeability [31], loss of K^+ selectivity [32,33], significantly lower analgesia compared with wildtype mice [3], and lack of activating effects of ethanol [34]. The *Kcnj6* gene orthologs might be under purifying selection over many generations of the species, including human and mouse, because of the profound functional constraints attributable to the importance of these orthologs in these organisms.

The A/A genotype in the A1032G SNP was significantly associated with increased postoperative analgesic requirements in our study. The G allele appears to be dominant in mediating the transmission of intensified opioid signaling compared with the A allele. However, this particular SNP is synonymous and causes no amino acid change; therefore, the protein structure encoded by this gene may not be altered by this SNP. Nevertheless, local structural difference in the 1023–1059 position was observed between the sequences, including 1032A and 1032G, in our prediction of the *KCNJ6* mRNA secondary structure (Figure S1). Whereas the 1032A mRNA formed an interior loop, a hairpin loop, and a 6 bp helix, the 1032G mRNA formed a bulge loop as well as an interior loop, a hairpin loop, and a 7 bp helix in the local structure. Although the role of this difference in gene function remains to be determined, the SNP may actually influence mRNA expression level. Indeed, recent studies measuring allelic expression imbalances [35] have demonstrated that even a synonymous SNP could affect mRNA and protein levels [36], possibly by altering mRNA stability and protein synthesis [37]. Similar mRNA and protein levels, but altered conformations, were found for synonymous polymorphisms [38].

To further infer the precise mechanism underlying the increased requirements for rescue analgesics in the A/A subjects in the A1032G SNP, we compared the relative *KCNJ6* mRNA expression level between the genotype subgroups of the SMRI samples in the real-time qPCR. A significant difference in expression level was observed between the A/A genotype and the combined A/G and G/G genotypes, consistent with the results of the association study, in which only the subjects with the A/A genotype in this SNP demonstrated significantly higher requirements for rescue analgesics than the other genotypes. The 1032A/A subjects required more analgesics, probably because of lower *KCNJ6* gene expression levels and consequently insufficient analgesic effects.

We do not have any evidence to explain how the −1250G/1032A haplotype contributes to increased requirements for rescue analgesics compared with other haplotypes. One might infer that the G-1250A SNP in the putative regulatory region could be related to some moderate functional alteration, and the −1250G and 1032A alleles could be risk factors for decreased sensitivity to analgesics. Both alleles might combine synergistically to cause profound decreases in sensitivity to analgesics. Future functional studies focusing on both the G-1250A and A1032G SNPs are required to investigate this hypothesis.

In conclusion, the A/A genotype in the *KCNJ6* A1032G SNP and −1250G/1032A haplotype were significantly associated with increased analgesic requirements after major open abdominal surgery. Furthermore, *KCNJ6* gene expression levels in the 1032A/A subjects was significantly decreased compared with the 1032A/G and 1032G/G subjects. Although the association might be restricted to the Japanese population, and the mechanism by which individual sensitivity to postoperative analgesics is altered by the G-1250A and A1032G SNPs remains to be fully elucidated, the outcome indicates that the A1032G SNP and G-1250A/A1032G haplotype could serve as markers that predict increased analgesic requirements. Our findings will provide valuable information to better modulate individual analgesic dosages required to achieve satisfactory pain control and open new avenues for personalized pain treatment.

Supporting Information

Table S1 The clinical data of the subjects stratified by genotype
Found at: doi:10.1371/journal.pone.0007060.s001 (0.12 MB DOC)

Figure S1 Predicted secondary structure for the KCNJ6 mRNA based on the nucleotide sequences of the GenBank database (accession number: NM_002240.2). The sequences for *KCNJ6* mRNA position 1012–1072 are presented for the 1032A (A) and 1032G (B) mRNA. The numbers next to the sequences indicate relative positions from position 982.
Found at: doi:10.1371/journal.pone.0007060.s002 (0.99 MB TIF)

Acknowledgments

We acknowledge Mr. Michael Arends for his assistance with editing the manuscript. We are grateful to the volunteers for their participation in this study and the anesthesiologists and surgeons at Research Hospital, Institute of Medical Science, The University of Tokyo, and Toho University Sakura Medical Center for collecting clinical data. We thank the Stanley Medical Research Institute for providing SMRI samples.

Author Contributions

Conceived and designed the experiments: DN SK NS IS MH KI. Performed the experiments: DN JH. Analyzed the data: DN YO. Contributed reagents/materials/analysis tools: DN YO WH JH. Wrote the paper: DN MH KI. Collection of DNA: YO KI. Collection of clinical data and DNA: MN RK YS MT MH.

References

1. Ikeda K, Ide S, Han W, Hayashida M, Uhl GR, et al. (2005) How individual sensitivity to opiates can be predicted by gene analyses. Trends Pharmacol Sci 26: 311–317.
2. Coulbault L, Beaussier M, Verstuyft C, Weickmans H, Dubert L, et al. (2006) Environmental and genetic factors associated with morphine response in the postoperative period. Clin Pharmacol Ther 79: 316–324.
3. Ikeda K, Kobayashi T, Kumanishi T, Yano R, Sora I, et al. (2002) Molecular mechanisms of analgesia induced by opioids and ethanol: is the GIRK channel one of the keys? Neurosci Res 44: 121–131.
4. Smith SB, Marker CL, Perry C, Liao G, Sotocinal SG, et al. (2008) Quantitative trait locus and computational mapping identifies *Kcnj9* (GIRK3) as a candidate gene affecting analgesia from multiple drug classes. Pharmacogenet Genomics 18: 231–241.
5. Kobayashi T, Ikeda K (2006) G protein-activated inwardly rectifying potassium channels as potential therapeutic targets. Curr Pharm Des 12: 4513–4523.
6. Marker CL, Lujan R, Loh HH, Wickman K (2005) Spinal G-protein-gated potassium channels contribute in a dose-dependent manner to the analgesic effect of μ- and δ- but not κ-opioids. J Neurosci 25: 3551–3559.
7. Marker CL, Lujan R, Loh HH, Wickman K (2005) Spinal G-protein-gated potassium channels contribute in a dose-dependent manner to the analgesic effect of μ- and δ- but not κ-opioids. J Neurosci 25: 3551–3559.
8. Marker CL, Stoffel M, Wickman K (2004) Spinal G-protein-gated K^+ channels formed by GIRK1 and GIRK2 subunits modulate thermal nociception and contribute to morphine analgesia. J Neurosci 24: 2806–2812.
9. Jelacic TM, Kennedy ME, Wickman K, Clapham DE (2000) Functional and biochemical evidence for G-protein-gated inwardly rectifying K^+ (GIRK) channels composed of GIRK2 and GIRK3. J Biol Chem 275: 36211–36216.
10. Kobayashi T, Ikeda K, Ichikawa T, Abe S, Togashi S, et al. (1995) Molecular cloning of a mouse G-protein-activated K^+ channel (mGIRK1) and distinct distributions of three GIRK (GIRK1, 2 and 3) mRNAs in mouse brain. Biochem Biophys Res Commun 208: 1166–1173.
11. Wickman K, Karschin C, Karschin A, Picciotto MR, Clapham DE (2000) Brain localization and behavioral impact of the G-protein-gated K^+ channel subunit GIRK4. J Neurosci 20: 5608–5615.
12. Ikeda K, Kobayashi T, Kumanishi T, Niki H, Yano R (2000) Involvement of G-protein-activated inwardly rectifying K^+ (GIRK) channels in opioid-induced analgesia. Neurosci Res 38: 113–116.
13. Blednov YA, Stoffel M, Alva H, Harris RA (2003) A pervasive mechanism for analgesia: activation of GIRK2 channels. Proc Natl Acad Sci U S A 100: 277–282.
14. Marker CL, Cintora SC, Roman MI, Stoffel M, Wickman K (2002) Hyperalgesia and blunted morphine analgesia in G protein-gated potassium channel subunit knockout mice. Neuroreport 13: 2509–2513.
15. Mitrovic I, Margeta-Mitrovic M, Bader S, Stoffel M, Jan LY, et al. (2003) Contribution of GIRK2-mediated postsynaptic signaling to opiate and α_2-adrenergic analgesia and analgesic sex differences. Proc Natl Acad Sci U S A 100: 271–276.
16. Sakura H, Bond C, Warren-Perry M, Horsley S, Kearney L, et al. (1995) Characterization and variation of a human inwardly-rectifying-K-channel gene (KCNJ6): a putative ATP-sensitive K-channel subunit. FEBS Lett 367: 193–197.
17. Stoffel M, Espinosa R, 3rd, Powell KL, Philipson LH, Le Beau MM, et al. (1994) Human G-protein-coupled inwardly rectifying potassium channel (GIRK1) gene (*KCNJ3*): localization to chromosome 2 and identification of a simple tandem repeat polymorphism. Genomics 21: 254–256.
18. Yasuda K, Sakura H, Mori Y, Iwamoto K, Shimokawa K, et al. (1995) No evidence for mutations in a putative subunit of the β-cell ATP-sensitive potassium channel (K-ATP channel) in Japanese NIDDM patients. Biochem Biophys Res Commun 211: 1036–1040.
19. Hayashida M, Nagashima M, Satoh Y, Katoh R, Tagami M, et al. (2008) Analgesic requirements after major abdominal surgery are associated with *OPRM1* gene polymorphism genotype and haplotype. Pharmacogenomics 9: 1605–1616.
20. Carlson CS, Eberle MA, Rieder MJ, Smith JD, Kruglyak L, et al. (2003) Additional SNPs and linkage-disequilibrium analyses are necessary for whole-genome association studies in humans. Nat Genet 33: 518–521.
21. Carlson CS, Eberle MA, Rieder MJ, Yi Q, Kruglyak L, et al. (2004) Selecting a maximally informative set of single-nucleotide polymorphisms for association analyses using linkage disequilibrium. Am J Hum Genet 74: 106–120.
22. de Bakker PI, Yelensky R, Pe'er I, Gabriel SB, Daly MJ, et al. (2005) Efficiency and power in genetic association studies. Nat Genet 37: 1217–1223.
23. Barrett JC, Fry B, Maller J, Daly MJ (2005) Haploview: analysis and visualization of LD and haplotype maps. Bioinformatics 21: 263–265.
24. Gabriel SB, Schaffner SF, Nguyen H, Moore JM, Roy J, et al. (2002) The structure of haplotype blocks in the human genome. Science 296: 2225–2229.
25. Zuker M (2003) Mfold web server for nucleic acid folding and hybridization prediction. Nucleic Acids Res 31: 3406–3415.
26. Faul F, Erdfelder E, Lang AG, Buchner A (2007) G*Power 3: a flexible statistical power analysis program for the social, behavioral, and biomedical sciences. Behav Res Methods 39: 175–191.
27. Purcell S, Neale B, Todd-Brown K, Thomas L, Ferreira MA, et al. (2007) PLINK: a tool set for whole-genome association and population-based linkage analyses. Am J Hum Genet 81: 559–575.
28. Benjamini Y, Hochberg Y (1995) Controlling the false discovery rate: a practical and powerful approach to multiple testing. J R Statist Soc B 57: 289–300.
29. Cohen J (1977) Statistical power analysis for the behavioral sciences (revised edition). New York: Academic Press.
30. Rakic P, Sidman RL (1973) Weaver mutant mouse cerebellum: defective neuronal migration secondary to abnormality of Bergmann glia. Proc Natl Acad Sci U S A 70: 240–244.
31. Patil N, Cox DR, Bhat D, Faham M, Myers RM, et al. (1995) A potassium channel mutation in weaver mice implicates membrane excitability in granule cell differentiation. Nat Genet 11: 126–129.
32. Navarro B, Kennedy ME, Velimirovic B, Bhat D, Peterson AS, et al. (1996) Nonselective and Gβγ-insensitive weaver K^+ channels. Science 272: 1950–1953.
33. Tong Y, Wei J, Zhang S, Strong JA, Dlouhy SR, et al. (1996) The weaver mutation changes the ion selectivity of the affected inwardly rectifying potassium channel GIRK2. FEBS Lett 390: 63–68.
34. Kobayashi T, Ikeda K, Kojima H, Niki H, Yano R, et al. (1999) Ethanol opens G-protein-activated inwardly rectifying K^+ channels. Nat Neurosci 2: 1091–1097.
35. Yan H, Yuan W, Velculescu VE, Vogelstein B, Kinzler KW (2002) Allelic variation in human gene expression. Science 297: 1143.
36. Zhang Y, Wang D, Johnson AD, Papp AC, Sadee W (2005) Allelic expression imbalance of human mu opioid receptor (OPRM1) caused by variant *A118G*. J Biol Chem 280: 32618–32624.

37. Duan J, Wainwright MS, Comeron JM, Saitou N, Sanders AR, et al. (2003) Synonymous mutations in the human dopamine receptor D2 (DRD2) affect mRNA stability and synthesis of the receptor. Hum Mol Genet 12: 205–216.
38. Kimchi-Sarfaty C, Oh JM, Kim IW, Sauna ZE, Calcagno AM, et al. (2007) A "silent" polymorphism in the *MDR1* gene changes substrate specificity. Science 315: 525–528.
39. Kalso E, Vainio A (1990) Morphine and oxycodone hydrochloride in the management of cancer pain. Clin Pharmacol Ther 47: 639–646.
40. Klinck JR, Lindop MJ (1982) Epidural morphine in the elderly: a controlled trial after upper abdominal surgery. Anaesthesia 37: 907–912.
41. Hoskin PJ, Hanks GW (1991) Opioid agonist-antagonist drugs in acute and chronic pain states. Drugs 41: 326–344.
42. Bahar M, Rosen M, Vickers MD (1985) Self-administered nalbuphine, morphine and pethidine: comparison, by intravenous route, following cholecystectomy. Anaesthesia 40: 529–532.
43. Pathak KS, Brown RH, Nash CL Jr, Cascorbi HF (1983) Continuous opioid infusion for scoliosis fusion surgery. Anesth Analg 62: 841–845.
44. Basar H, Yilmaz E, Ozcan S, Buyukkocak U, Sari F, et al. (2003) Four analgesic techniques for shockwave lithotripsy: eutectic mixture local anesthetic is a good alternative. J Endourol 17: 3–6.
45. Ozcan S, Yilmaz E, Buyukkocak U, Basar H, Apan A (2002) Comparison of three analgesics for extracorporeal shock wave lithotripsy. Scand J Urol Nephrol 36: 281–285.
46. Buchanan WW, Kassam YB (1986) European experience with flurbiprofen: a new analgesic/anti-inflammatory agent. Am J Med 80: 145–152.
47. Sunshine S, Olson NZ (1994) Nonnarcotic analgesics. In: Wall PD, Melzack R, Bonica JJ, eds. Textbook of pain, 3rd edn. Edinburgh: Churchill Livingstone. pp 923–942.

Pregnenolone Sulfate Potentiates the Inwardly Rectifying K^+ Channel Kir2.3

Toru Kobayashi[1]*, Kazuo Washiyama[1], Kazutaka Ikeda[2]

1 Department of Molecular Neuropathology, Brain Research Institute, Niigata University, Chuo-ku, Niigata, Niigata, Japan, 2 Division of Psychobiology, Tokyo Institute of Psychiatry, Setagaya, Tokyo, Japan

Abstract

Background: Neurosteroids have various physiological and neuropsychopharmacological effects. In addition to the genomic effects of steroids, some neurosteroids modulate several neurotransmitter receptors and channels, such as *N*-methyl-D-aspartate receptors, γ-aminobutyric acid type A ($GABA_A$) receptors, and σ_1 receptors, and voltage-gated Ca^{2+} and K^+ channels. However, the molecular mechanisms underlying the various effects of neurosteroids have not yet been sufficiently clarified. In the nervous system, inwardly rectifying K^+ (Kir) channels also play important roles in the control of resting membrane potential, cellular excitability and K^+ homeostasis. Among constitutively active Kir2 channels in a major Kir subfamily, Kir2.3 channels are expressed predominantly in the forebrain, a brain area related to cognition, memory, emotion, and neuropsychiatric disorders.

Methodology/Principal Findings: The present study examined the effects of various neurosteroids on Kir2.3 channels using the *Xenopus* oocyte expression assay. In oocytes injected with Kir2.3 mRNA, only pregnenolone sulfate (PREGS), among nine neurosteroids tested, reversibly potentiated Kir2.3 currents. The potentiation effect was concentration-dependent in the micromolar range, and the current-voltage relationship showed inward rectification. However, the potentiation effect of PREGS was not observed when PREGS was applied intracellularly and was not affected by extracellular pH conditions. Furthermore, although Kir1.1, Kir2.1, Kir2.2, and Kir3 channels were insensitive to PREGS, in oocytes injected with Kir2.1/Kir2.3 or Kir2.2/Kir2.3 mRNA, but not Kir2.1/Kir2.2 mRNA, PREGS potentiated Kir currents. These potentiation properties in the concentration-response relationships were less potent than for Kir2.3 channels, suggesting action of PREGS on Kir2.3-containing Kir2 heteromeric channels.

Conclusions/Significance: The present results suggest that PREGS acts as a positive modulator of Kir2.3 channels. Kir2.3 channel potentiation may provide novel insights into the various effects of PREGS.

Citation: Kobayashi T, Washiyama K, Ikeda K (2009) Pregnenolone Sulfate Potentiates the Inwardly Rectifying K^+ Channel Kir2.3. PLoS ONE 4(7): e6311. doi:10.1371/journal.pone.0006311

Editor: Michael N. Nitabach, Yale School of Medicine, United States of America

Received April 14, 2009; **Accepted** June 23, 2009; **Published** July 21, 2009

Funding: This work was supported by research grants from the Ministry of Education, Culture, Sports Science and Technology of Japan and the Ministry of Health, Labour and Welfare of Japan. The funders had no role in study design, data collection and analysis, decision to publish, or preparation of the manuscript.

Competing Interests: The authors have declared that no competing interests exist.

* E-mail: torukoba@bri.niigata-u.ac.jp

Introduction

Neurosteroids are synthesized by neurons and glial cells in the central and peripheral nervous system from cholesterol or other blood-borne steroidal precursors [1,2]. In addition to the genomic effects of steroids via intracellular steroid receptors, some steroids modulate the functions of several neurotransmitter receptors and channels, namely γ-aminobutyric acid type A ($GABA_A$) receptors, *N*-methyl-D-aspartate (NMDA) receptors, serotonin (5-hydroxytryptamine, 5-HT) subtype 3 ($5\text{-}HT_3$) receptors, and σ_1 receptors [3], voltage-gated Ca^{2+} and K^+ channels [4,5], and transient receptor potential M3 channels [6], possibly leading to modulation of neuronal excitability. Steroids with these properties are referred to as neuroactive steroids independently of their origin [3]. Neurosteroids have been shown to have a variety of neuropsychopharmacological effects, such as neuroprotective, memory-enhancing, sedative, anxiolytic, sleep-modulating, antidepressant, anticonvulsant and anesthetic effects [2,3]. However, the molecular mechanisms underlying the various effects of neurosteroids have not yet been sufficiently clarified.

Inwardly rectifying K^+ (Kir) channels play important roles in the control of resting membrane potential, cellular excitability and K^+ homeostasis in the nervous system and various peripheral tissues [7]. Among seven Kir subfamilies, members of Kir2 channels in a major Kir subfamily are characterized by strong inward rectification and constitutive activity and are present in various cells, including neurons, glial cells, cardiac and skeletal myocytes, epithelial cells, and macrophages [8]. Four Kir2 channel members have been identified in mammals [9–13]. In the nervous system, Kir2.1 channels are expressed widely but weakly in most brain regions. Kir2.2 channels are expressed mainly in the cerebellum. Kir2.3 channels are expressed predominantly in the forebrain [14,15]. Kir2.4 channels are expressed predominantly in motoneurons of the brainstem [13]. Among Kir2 channels, Kir2.3 channels in the forebrain may be related to cognition, memory, emotion and neuropsychiatric disorders. Therefore, endogenous modulators of Kir2.3 channels may induce various physiological and neuropsychopharmacological effects. In the present study, we investigated the effects of various neurosteroids on Kir2.3 channels using the *Xenopus* oocyte expression assay.

Results

PREGS potentiates Kir2.3 channels

In *Xenopus* oocytes injected with Kir2.3 mRNA, inward currents through the expressed Kir 2.3 channels were observed at a holding potential of −70 mV in an hK solution containing 96 mM K^+ (Fig. 1A). Extracellular application of 30 μM pregnenolone sulfate (PREGS) reversibly potentiated Kir2.3 currents (Fig. 1A). The current responses to an additional 50 μM PREGS during application of 3 mM Ba^{2+}, which blocks Kir channels, were not significant (1.5±1.0 nA, less than 1% of the 3 mM Ba^{2+}-sensitive current component, $n=4$; Fig. 1A). The 3 mM Ba^{2+}-sensitive current components in oocytes expressing Kir2.3 channels (684.7±79.2 nA, $n=25$) are considered to correspond to the magnitudes of Kir2.3 currents in oocytes expressing Kir2.3 channels [11]. PREGS produced no significant response in the K^+-free ND98 solution containing 98 mM Na^+ instead of the hK solution (5.7±2.0 nA at 50 μM, $n=4$), suggesting that the PREGS-induced currents show K^+ selectivity. In uninjected oocytes, 300 μM PREGS and 3 mM Ba^{2+} produced no significant response (less than 5 nA and 3.2±2.5 nA, respectively, $n=5$; Fig. 1A) compared with oocytes injected with Kir2.3 mRNA, suggesting no significant effect of PREGS and Ba^{2+} on intrinsic oocyte channels. Additionally, application of dimethyl sulfoxide (DMSO), the solvent vehicle, at the highest concentration (0.3%) produced no significant response in oocytes injected with Kir2.3 mRNA ($n=4$; data not shown). In contrast, 100 μM of the other neurosteroids tested: PREG, dehydroepiandrosterone (DHEA), DHEAS, progesterone, 17β-estradiol, corticosterone, 5α-pregnan-3α-ol-20-one (3α-OH-DHP, also known as allopregnanolone) and 3α, 21-dihydroxy-5α-pregnan-20-one (also known as tetrahydrodeoxycorticosterone, THDOC), produced no significant current responses in oocytes expressing Kir2.3 channels (less than 2% change of the 3 mM Ba^{2+}-sensitive current component, with the exception of DHEAS with only 5.6±2.6% potentiation, $n\geq4$; Fig. 1B). The results suggest that Kir2.3 channels are potentiated specifically by PREGS among various neurosteroids.

Characteristics of Kir2.3 channel potentiation by PREGS

The potentiation of Kir2.3 channels by PREGS was concentration-dependent at micromolar concentrations, with a concentration of PREGS that produces 50% of the maximal effect (EC_{50}) of 15.6±0.9 μM and a Hill coefficient (n_H) of 1.43±0.03 ($n=6$, Fig. 2A). The amplitudes of 30 μM PREGS-potentiated Kir2.3 currents were highly correlated with those of 3 mM Ba^{2+}-sensitive current components (Fig. 2B), suggesting that the effects of PREGS may be associated with Kir2.3 channel expression levels.

Furthermore, instantaneous Kir2.3 currents elicited by the voltage step to −100 mV from a holding potential of 0 mV were enhanced in the presence of 30 μM PREGS applied for 3.5 min (Fig. 2C). The percentage potentiation of the steady-state Kir2.3 current at the end of the voltage step by PREGS was not significantly different from that of the instantaneous current (paired *t*-test, $P>0.05$; $n=6$ at −40, −60, −80, −100 and −120 mV, respectively). These results suggest that the channels were potentiated by PREGS primarily at the holding potential of 0 mV and in a time-independent manner during each voltage pulse. Similarly to 3 mM Ba^{2+}-sensitive currents corresponding to Kir2.3 currents, PREGS-induced currents in oocytes expressing Kir2.3 channels increased with negative membrane potentials, and the current-voltage relationships showed inward rectification (Fig. 2D), indicating a characteristic of Kir currents. Furthermore, the PREGS-induced current did not change the reversal potential. These results suggest that PREGS potentiates the function of Kir2.3 channels.

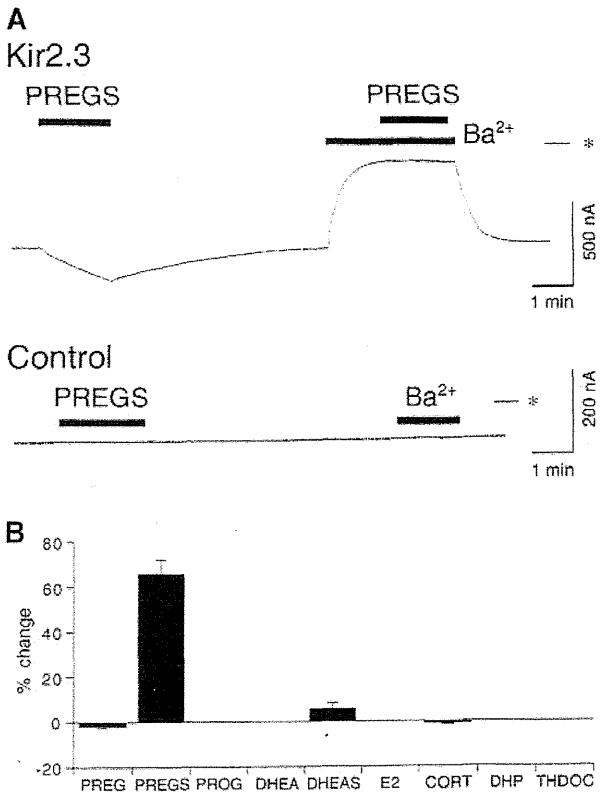

Figure 1. Effects of pregnenolone sulfate (PREGS) on Kir2.3 channels expressed in *Xenopus* oocytes. (A) Upper row, in an oocyte injected with Kir2.3 mRNA, current responses to 30 μM PREGS and to 50 μM PREGS in the presence of 3 mM Ba^{2+} are shown. Lower row, in an uninjected oocyte, no significant current responses to 300 μM PREGS and 3 mM Ba^{2+} are shown. Current responses were measured at a membrane potential of −70 mV in an hK solution containing 96 mM K^+. Asterisks show the zero current level. Horizontal bars show the duration of application. (B) Effects of various neurosteroids: PREG, PREGS, DHEA, DHEAS, progesterone (PROG), 17β-estradiol (E2), corticosterone (CORT), 3α-OH-DHP and THDOC, on Kir2.3 channels. The magnitudes of the effect of 100 μM neurosteroids on Kir2.3 channels were normalized to the 3 mM Ba^{2+}-sensitive current components in oocytes expressing Kir2.3 channels ($n\geq4$ for each steroid). Data are expressed as mean±SEM.
doi:10.1371/journal.pone.0006311.g001

The effects of intracellular PREGS in oocytes expressing Kir2.3 channels were also examined. The 3 mM Ba^{2+}-sensitive current components corresponding to the magnitudes of Kir2.3 currents were not significantly affected by intracellularly applied PREGS (88.4±12.1% of untreated control, $P>0.05$, paired *t*-test, $n=4$; Fig. 3A), and extracellular application of 50 μM PREGS after the injection similarly potentiated Kir currents ($P>0.05$, paired *t*-test, $n=4$; Fig. 3B). These results suggest that the potentiation effect of PREGS was not caused by its intracellular action.

The chemical structure of PREGS shares the structural moiety of PREG and DHEAS [3]. However, 30 μM PREGS-induced Kir2.3 currents were not significantly different from those in the presence of either 100 μM PREG or 100 μM DHEAS (105.9±11.4% and 99.8±8.9% of control, respectively, $P>0.05$, $n=4$, paired *t*-test; Fig. 4), suggesting that PREG and DHEAS have no significant antagonist effect on the potentiation of Kir2.3 channels by PREGS.

Kir2.3 channels are modulated by extracellular pH [16–18]. We examined whether changes in pH would alter the effects of

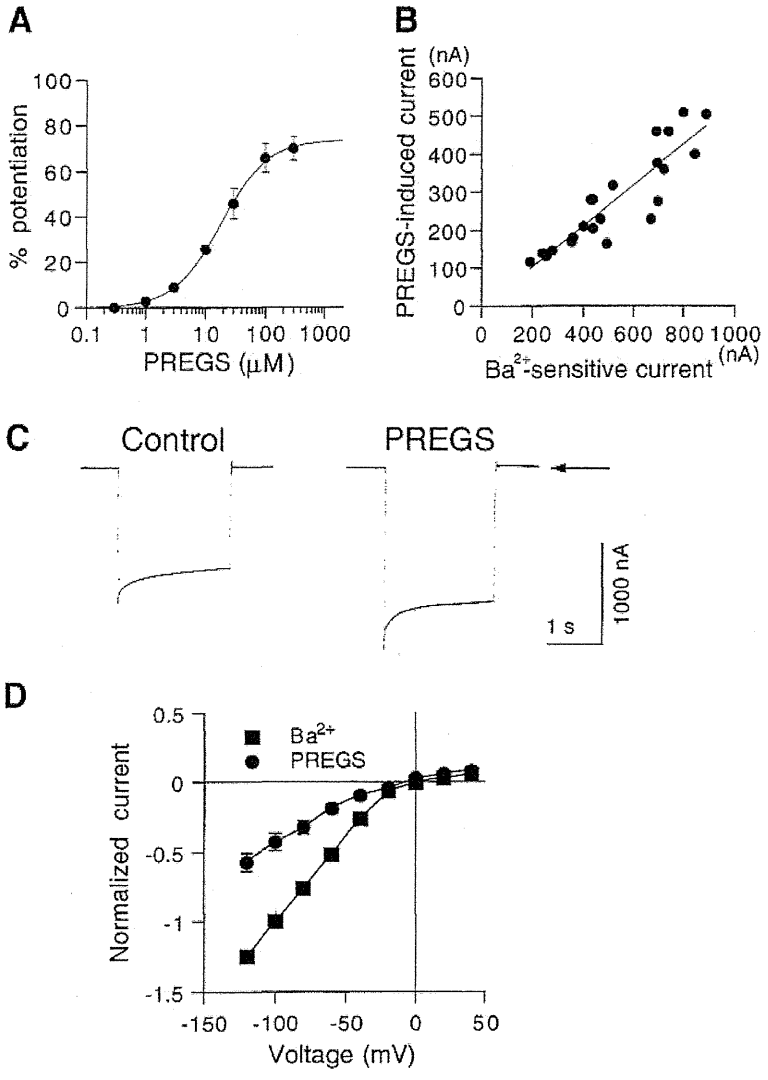

Figure 2. Characteristics of Kir2.3 channel potentiation by PREGS. (A) Concentration-dependent effect of PREGS on Kir2.3 channels. The magnitudes of Kir2.3 currents potentiated by PREGS were normalized to the 3 mM Ba^{2+}-sensitive current components in *Xenopus* oocytes expressing Kir2.3 channels (554.0±79.9 nA, $n=6$). Data are expressed as mean±SEM of the percentage responses. (B) Correlation between amplitudes of current response to 30 μM PREGS and amplitudes of the 3 mM Ba^{2+}-sensitive current components in oocytes expressing Kir2.3 channels. The correlation coefficient was 0.894 ($P<0.05$, $n=22$, regression analysis). Current responses were measured at a membrane potential of −70 mV in an hK solution containing 96 mM K^+. (C) Representative Kir2.3 currents elicited by a voltage step to −100 mV for 2 s from a holding potential of 0 mV in the presence or absence of 30 μM PREGS in an oocyte injected with Kir2.3 mRNA. Arrow indicates the zero current level. (D) Current-voltage relationships of 3 mM Ba^{2+}-sensitive currents and 30 μM PREGS-enhanced currents in oocytes expressing Kir2.3 channels. Current responses were normalized to the 3 mM Ba^{2+}-sensitive current component measured at a membrane potential of −100 mV (1510.0±209.9 nA, $n=6$).
doi:10.1371/journal.pone.0006311.g002

PREGS on Kir2.3 channels expressed in *Xenopus* oocytes. In oocytes injected with Kir2.3 mRNA, Kir2.3 currents decreased with a decrease in extracellular pH (51.9±7.9% of the 3 mM Ba^{2+}-sensitive current components at pH 7.4 for pH 6.0, $n=6$; and 167.6±22.1% of those at pH 7.4 for pH 9.0, $n=6$) as reported in previous studies [16–18]. However, the concentration-response relationships for the potentiation effects of PREGS were not significantly affected by pH 6.0, 7.4 and 9.0 (no significant pH × PREGS interaction, $P>0.05$, two-way ANOVA; $P>0.05$ at each concentration, Tukey-Kramer *post hoc* test; Fig. 5). These results suggest that the degree of potentiation of Kir2.3 channels by PREGS may be similar even under pathological pH conditions.

Selective potentiation of Kir2.3 channels by PREGS

We also examined the effects of PREGS on other Kir channels (i.e., Kir1.1, an ATP-regulated Kir channel; Kir2.1 and Kir2.2, constitutively active Kir channels; Kir3, a G protein-activated Kir channel [7]). However, in oocytes injected with mRNA for Kir1.1, Kir2.1, Kir2.2, or Kir3.1/Kir3.2 channels, 100 μM PREGS produced no significant current response (3.5±0.4, 7.2±3.7, 4.0±2.5, and 0.8±1.6% change of the 3 mM Ba^{2+}-sensitive current components: 820.7±190.8 nA for Kir1.1, 538.0±130.9 nA for Kir2.1, 1518.3±276.4 nA for Kir2.2, and 1043.5±166.0 nA for Kir3.1/Kir3.2, respectively, $n\geq4$; Fig. 6). These results suggest that PREGS selectively potentiates Kir2.3 channels.

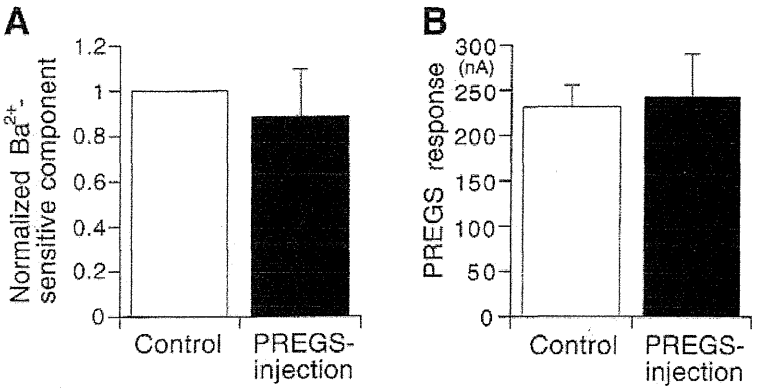

Figure 3. Effect of intracellular PREGS in *Xenopus* oocytes expressing Kir2.3 channels. (A) Comparison of basal Kir2.3 currents before and after PREGS injection in oocytes expressing Kir2.3 channels. The amplitude of Kir2.3 currents was normalized to the amplitude of 3 mM Ba^{2+}-sensitive current components before PREGS injection. (B) Comparison of 50 μM PREGS-induced Kir2.3 currents before and after PREGS injection. Data are expressed as mean±SEM.
doi:10.1371/journal.pone.0006311.g003

Effects of PREGS on Kir2 heteromeric channels

Recent studies have shown that Kir2 channel subunits can form functional heteromeric channels in the *Xenopus* oocyte expression system [19,20]. We examined the effects of PREGS on Kir2 heteromeric channels. In oocytes injected with mRNA for Kir2.1/Kir2.3 or Kir2.2/Kir2.3, PREGS concentration-dependently potentiated Kir currents (respective EC50 and n_H: 41.0±9.4 μM and 1.40±0.23 for Kir2.1/Kir2.3, $n=6$; 27.5±5.0 μM and 1.07±0.07 for Kir2.2/Kir2.3, $n=9$; Fig. 7), whereas PREGS had no significant current response in oocytes injected with Kir2.1/Kir2.2 mRNA (1.3±1.3% inhibition of the 3 mM Ba^{2+}-sensitive current components, $n=5$). The potentiation properties of PREGS in the normalized concentration-response relationships were less potent for Kir2.1/Kir2.3 and Kir2.2/Kir2.3 than for Kir2.3 channels (EC50: $P<0.05$, one-way ANOVA; significant difference between Kir2.1/Kir2.3 and Kir2.3, $P<0.05$, Tukey-Kramer *post hoc* test; and significant channel-type × PREGS

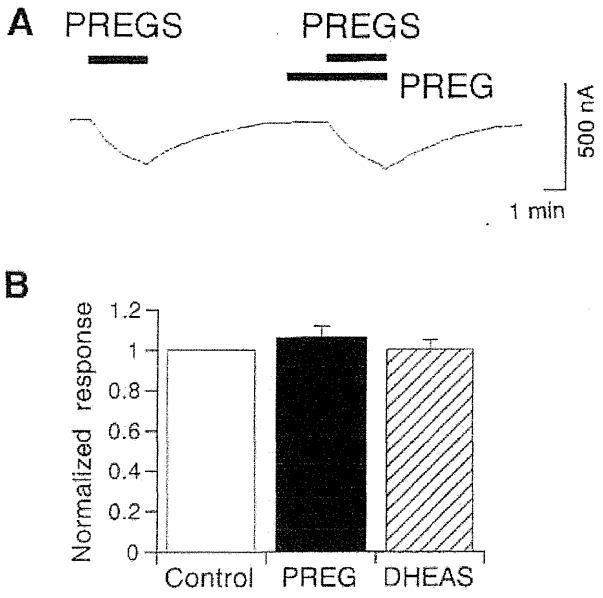

Figure 4. Effects of PREG and DHEAS on PREGS-induced Kir2.3 currents. (A) Representative current responses to 30 μM PREGS and to 30 μM PREGS in the presence of 100 μM PREG in a *Xenopus* oocyte expressing Kir2.3 channels. Current responses were measured at a membrane potential of −70 mV in an hK solution containing 96 mM K^+. (B) Comparison of PREGS-induced Kir2.3 currents in the presence or absence of PREG or DHEAS. Concentrations of PREGS, PREG, and DHEAS were 30, 100, and 100 μM, respectively. Current responses to PREGS in the presence of PREG or DHEAS were normalized to the amplitude of PREGS-induced currents in the absence of PREG or DHEAS (control). Data are expressed as mean±SEM.
doi:10.1371/journal.pone.0006311.g004

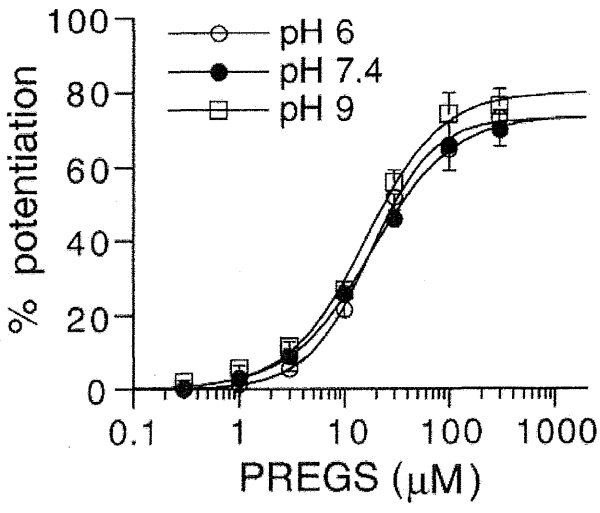

Figure 5. Concentration-response relationships for potentiation of Kir2.3 channels by PREGS at different pH values. The magnitudes of potentiation of Kir2.3 currents by PREGS in oocytes expressing Kir2.3 channels were normalized to the 3 mM Ba^{2+}-sensitive current components, which were 426.9.6±41.4 nA (pH 6.0), 554.0±79.9 nA (pH 7.4) and 729.2±36.6 nA (pH 9.0). The EC_{50} and n_H values were 16.1±1.2 μM and 1.44±0.07 (pH 6.0, $n=10$), 15.6±0.9 μM and 1.43±0.03 (pH 7.4, $n=6$), and 17.1±1.5 μM and 0.70±0.03 (pH 9.0, $n=8$), respectively. Current responses were measured at a membrane potential of −70 mV in an hK solution containing 96 mM K^+. Data are expressed as mean±SEM of the percentage responses.
doi:10.1371/journal.pone.0006311.g005

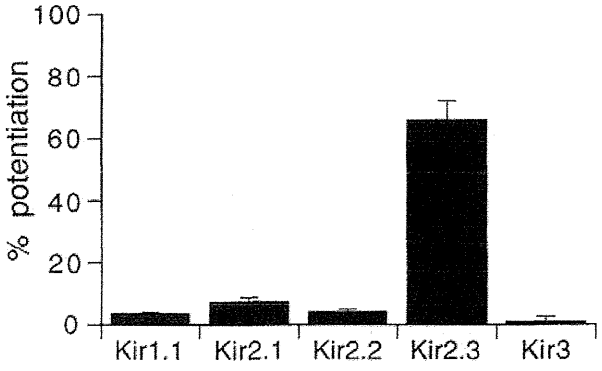

Figure 6. Comparison of the effects of PREGS on Kir1.1, Kir2.1, Kir2.2, Kir2.3, and Kir3 channels expressed in *Xenopus* oocytes. The magnitudes of change in Kir currents by 100 μM PREGS were normalized to the 3 mM Ba^{2+}-sensitive current components. For Kir3 channels, oocytes expressing brain-type Kir3.1/Kir3.2 channels were used. Current responses were measured at a membrane potential of −70 mV in an hK solution containing 96 mM K^+. Data are expressed as mean±SEM.
doi:10.1371/journal.pone.0006311.g006

interaction, $P<0.05$, two-way ANOVA; $P<0.05$ at 30 μM, Tukey-Kramer *post hoc* test). The results suggest that PREGS may also potentiate Kir2.3-containing Kir2 heteromeric channels.

Discussion

In the present study, we demonstrated that PREGS potentiated the function of Kir2.3 channels at micromolar concentrations, whereas the eight other neurosteroids (i.e., PREG, DHEA, DHEAS, progesterone, 17β-estradiol, corticosterone, 3α-OH-DHP, and THDOC) had no significant effect on Kir2.3 channels. Kir1.1, Kir2.1, Kir2.2 and Kir3 channels in other members of the Kir channel family were insensitive to PREGS. These results suggest that the endogenous steroid PREGS may selectively act as a positive modulator of Kir2.3 channels. Furthermore, the effect of PREGS on Kir2.3 channels was not caused by intracellularly applied PREGS, and potentiation of Kir2.3 channels by extracellularly applied PREGS was readily reversible with washout. PREGS exists in a negatively charged form, and it could not readily permeate the cell membrane. Therefore, the effect of PREGS was unlikely to be caused by intracellular PREGS or by interactions with intracellular molecules, including phosphatidylinositol 4,5-bisphosphate (PIP_2) and long-chain fatty acids that activate Kir2.3 channels [21,22]. Additionally, PREG and DHEAS, whose structures are closely related to PREGS, had no significant effects on Kir2.3 channels or on PREGS-induced Kir2.3 potentiation, suggesting that the effect of PREGS is unlikely to be mediated by a nonspecific membrane-perturbation effect. These observations suggest that PREGS may act directly at Kir2.3 channels, and the site of action of PREGS on Kir2.3 channels may be extracellular or, at least, at a readily accessible site from the outside of the cell membrane. Moreover, the present study suggests that PREGS also potentiates Kir2 heteromeric channels containing Kir2.3 channel subunits. The Kir2.3 channel may be considered as a target site for PREGS.

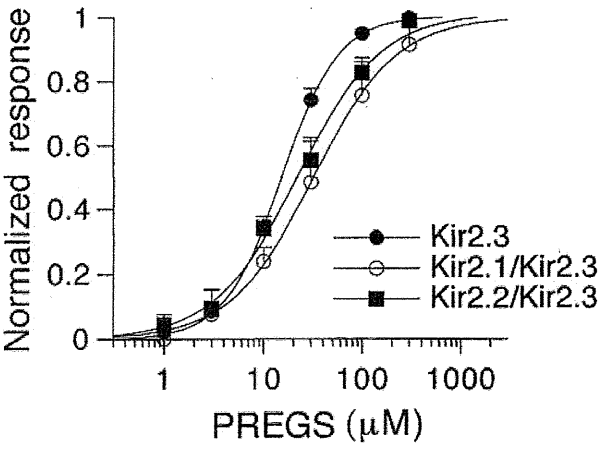

Figure 7. Comparison of the potentiation effects of PREGS on Kir2.3, Kir2.1/Kir2.3, and Kir2.2/Kir2.3 channels expressed in *Xenopus* oocytes. Responses to PREGS at different concentrations were normalized to the maximal response to PREGS. Current responses were measured at a membrane potential of −70 mV. Data are expressed as mean±SEM.
doi:10.1371/journal.pone.0006311.g007

Administration of PREGS has been shown to have antiamnesic, anxiolytic, antidepressant, neurogenesis, neuroprotective, proconvulsant, and antinociceptive effects [23–29] and prevent the development of tolerance and dependence to morphine and benzodiazepines [30,31]. PREGS at micromolar concentrations has also been shown to modulate the functions of several receptors and channels, namely $GABA_A$ receptors, glycine receptors, NMDA receptors, α-amino-3-hydroxy-5-methylisoxazole-4-propionic acid (AMPA) receptors, σ_1 receptors, voltage-gated Ca^{2+} and K^+ channels, and transient receptor potential M3 channels [3–6,27]. PREGS can cross the blood-brain barrier [32], and interactions of PREGS with these target sites are proposed to have important implications in the various effects of PREGS. Kir2.3 channels are highly expressed in neurons and some of oligodendroglial cells in the forebrain, such as the olfactory bulb, cerebral cortex, hippocampus and basal ganglia, and spinal cord [14,15,33,34], areas related to cognition, memory, emotion, nociception and drug addiction. Additionally, Kir2.3 channels colocalize with postsynaptic density-95 (PSD-95) in neuronal populations in the forebrain [35] and are localized at the postsynaptic membrane of excitatory synapses in the olfactory bulb [15], suggesting the existence of postsynaptic Kir2.3 channels. In the present study, PREGS potentiated Kir2.3 channels at micromolar concentrations. Because activation of Kir2.3 channels causes membrane hyperpolarization [36], PREGS may decrease excitability of neurons and glial cells in these regions. Furthermore, the distribution of Kir2.1, Kir2.2 and Kir2.3 subunits overlaps in some regions [14,33,34], suggesting the partial existence of Kir2 heteromeric channels. The present study suggests that PREGS also potentiates Kir2.3-containing Kir2 heteromeric channels. Therefore, Kir2.3 potentiation by PREGS might be involved in some of the various neuropsychopharmacological effects.

Bulk concentrations of PREGS in brain tissues have been estimated to be in the nanomolar range [37,38], or even lower [39,40]. However, the PREG synthase cytochrome P450 side-chain cleavage enzyme and hydroxysteroid sulfotransferase, which converts PREG to PREGS, are expressed in the brain [2], and these enzymes have been shown to colocalize in hippocampal neurons [38], suggesting local synthesis of PREGS. Furthermore, Mameli *et al.* [41] reported that a PREGS-like neurosteroid released from depolarized postsynaptic CA1 neurons increased the frequency of AMPA-mediated miniature excitatory postsynaptic currents via modulation of presynaptic NMDA receptors, with a magnitude equivalent to that caused by exogenously applied PREGS at 17 μM. This effect was blocked by anti-PREGS antibodies. These findings suggest that local concentrations of released PREGS around these neurons might be in the micromolar range.

Moreover, brain levels of neurosteroids, including PREGS, have been shown to be elevated under several pathological conditions, such as cerebral ischemia, epilepsy, stress, and drug addiction [3,42–46]. Altogether, Kir2.3 channels in the forebrain, including the hippocampus, might be potentiated by PREGS via paracrine and autocrine mechanisms under such conditions. Additionally, although PREG is structurally related to PREGS, PREG had no significant effect on Kir2.3 channels (Figs. 1B,4). Steroid sulfatase, which converts PREGS to PREG, has been identified in various brain regions [47–49]. Conversion between PREGS and PREG by sulfotransferase and steroid sulfatase might regulate the effect of PREGS on Kir2.3 channels in the brain.

Finally, Kir2.3 channels are also expressed in Schwann cells near the nodes of Ranvier in sciatic nerves, cardiomyocytes, and renal cortical collecting duct principal cells [50–52]. Typical plasma concentrations of PREGS have been reported to be 0.2 to 0.4 μM, although plasma concentrations of PREGS in some healthy subjects have been reported to be approximately 1 μM [53]. However, plasma PREGS levels can reach micromolar levels during pregnancy and in patients with 21-hydroxylase deficiency [54,55]. Elevated PREGS levels overlapped with the concentrations that were effective in potentiating Kir2.3 channels in the present study. Additionally, elevated plasma PREGS levels have been observed in patients with anxiety-depressive disorder, alcohol addiction, or hyperthyroidism [56–58]. Kir2.3 channels in the peripheral tissues may be potentiated by elevated PREGS concentrations in certain conditions. Potentiation of Kir2.3 channels by PREGS might affect the regulation of K^+ buffering in peripheral nerves, the control of cardiomyocyte excitability and K^+ homeostasis in the kidney. Interestingly, PREGS has been identified in sciatic nerves [59], and PREG has been identified in Schwann cells [60]. In sciatic nerves, Kir2.3 channels may also be potentiated by locally released PREGS. Further studies using local administration of PREGS and *in vitro* preparations, such as culture cells and brain slices, may advance our understanding of the physiological and pharmacological effects of PREGS on Kir2.3 channels in the nervous system, heart, and kidney. Kir2.3 channel potentiation may provide novel insights into the various effects of PREGS.

Materials and Methods

Compounds

PREG, PREGS, DHEA, DHEAS, progesterone, 17β-estradiol, corticosterone, 3α-OH-DHP, and THDOC were purchased from Sigma-Aldrich (St. Louis, MO, USA). PREGS was dissolved in distilled water or DMSO, and the others were dissolved in DMSO. The stock solution of each compound was stored at −30°C until use. Each compound was added to the perfusion solution in appropriate amounts immediately before the experiments.

Preparation of specific mRNA

Plasmids containing the entire coding sequences for the mouse Kir2.2 (GenBank accession number: AB035889), Kir2.3, Kir3.1, and Kir3.2 channel subunits were obtained as described previously [61–63]. The sequence of amino acids deduced from the nucleotide sequence of C57BL/6NJcl mouse Kir2.2 in the plasmid pSP35T revealed seven amino acids substitutions compared with BALB/c mouse Kir2.2 [12]. However, the substitutions were identical to those of rat Kir2.2, with the exception of a change from Phe to Leu at codon 255 [10]. Additionally, cDNAs for rat Kir1.1 in pSPORT and mouse Kir2.1 in pcDNA1 were generously provided by Drs. Steven C. Hebert and Lily Y. Jan, respectively [9,64]. The plasmid pSPKir2.2 was linearized by digestion with SacI, and the others were digested with the appropriate enzyme as described previously [9,62–64]. The specific mRNAs were synthesized *in vitro* using the mMESSAGE mMACHINE™ *In Vitro* Transcription Kit (Ambion, Austin, TX, USA).

Oocyte electrophysiology

Xenopus laevis oocytes (Stages V and VI) were isolated from adult female frogs (Copacetic, Soma, Aomori, Japan) that were anesthetized by immersion in water containing 0.15% tricaine (Sigma-Aldrich) as described previously [65]. All procedures for the care and treatment of animals were approved by Niigata University Institutional Animal Care and Use Committee in accordance with the National Institutes of Health guidelines. Oocytes were injected with mRNA for Kir1.1 (1 ng), Kir2.1 (0.5 ng), Kir2.2 (0.5 ng), Kir2.3 (1 ng), Kir2.1/Kir2.2, Kir2.1/Kir2.3, Kir2.2/Kir2.3 (each 0.5 ng), or Kir3.1/Kir3.2 combinations (each 0.3 ng) for brain-type Kir3 channels. Oocytes were incubated at 19°C in Barth's solution after treatment with 0.8 mg/ml collagenase and manually defolliculated. Whole-cell currents of the oocytes were recorded from 2 to 7 days after the injection with a conventional two-electrode voltage clamp [62,66]. The membrane potential was held at −70 mV, unless otherwise specified. Microelectrodes were filled with 3 M KCl. The oocytes were placed in a 0.05 ml narrow chamber and superfused continuously with a high-K^+ (hK) solution (composition in mM: KCl 96, NaCl 2, $MgCl_2$ 1, $CaCl_2$ 1.5 and HEPES 5, pH 7.4 with KOH) or a K^+-free high-Na^+ (ND98) solution (composition in mM: NaCl 98, $MgCl_2$ 1, $CaCl_2$ 1.5 and HEPES 5, pH 7.4 with NaOH). In the hK solution, the K^+ equilibrium potential was close to 0 mV, and the inward K^+ current flow through the Kir channels was observed at negative holding potentials [9,11,12,62,64]. For examining the effects of intracellular PREGS, 13.8 nl of 10 mM PREGS dissolved in distilled water containing 5% DMSO was injected into an oocyte using a Nanoliter injector (World Precision Instruments, Sarasota, FL, USA) as described previously [67]. The oocyte currents were then continuously recorded for approximately 30–40 min. Because the volume of the oocyte was approximately 1 μl, the intracellular concentration of PREGS was presumed to be approximately 136 μM. Furthermore, injection of the same volume of the solvent vehicle had no significant effect on Kir2.3 currents ($n = 4$). For analysis of concentration-response relationships, data were fitted to a standard logistic equation using KaleidaGraph (Synergy Software, Reading, PA, USA). EC_{50} and n_H values were obtained from the concentration-response relationships.

Data analyses

Data are expressed as mean±SEM, and n is the number of oocytes tested. Statistical analysis of differences between groups was performed using paired t-test, one-way analysis of variance (ANOVA), or two-way ANOVA followed by Tukey-Kramer *post hoc* test. Values of $P<0.05$ were considered statistically significant.

Acknowledgments

We are grateful to Dr. Kansaku Baba for his cooperation and Kazuo Kobayashi (Niigata University) for his assistance. We also thank Dr. Steven C. Hebert (Yale University) and Dr. Lily Y. Jan (University of California, San Francisco) for generously providing Kir1.1 cDNA and Kir2.1 cDNA, respectively.

Author Contributions

Conceived and designed the experiments: TK. Performed the experiments: TK. Analyzed the data: TK KW KI. Contributed reagents/materials/analysis tools: TK KW KI. Wrote the paper: TK KI.

References

1. Baulieu EE, Robel P, Schumacher M (2001) Neurosteroids: beginning of the story. Int Rev Neurobiol 46: 1–32.
2. Mellon SH, Griffin LD (2002) Neurosteroids: biochemistry and clinical significance. Trends Endocrinol Metabolism 13: 35–43.
3. Rupprecht R, Holsboer F (1999) Neuroactive steroids: mechanisms of action and neuropsychopharmacological perspectives. Trends Neurosci 22: 410–416.
4. ffrench-Mullen JMH, Danks P, Spence KT (1994) Neurosteroids modulate calcium currents in hippocampal CA1 neurons via a pertussis toxin-sensitive G-protein-coupled mechanism. J Neurosci 14: 1963–1977.
5. Wang Q, Wang L, Wardwell-Swanson (1998) Modulation of cloned human neuronal voltage-gated potassium channels (hKv1.1 and hKv2.1) by neurosteroids. Pflügers Arch 437: 49–55.
6. Wagner TFJ, Loch S, Lambert S, Straub I, Mannebach S, et al. (2008) Transient receptor potential M3 channels are ionotropic steroids in pancreatic β cells. Nat Cell Biol 10: 1421–1430.
7. Reimann F, Ashcroft FM (1999) Inwardly rectifying potassium channels. Curr Opin Cell Biol 11: 503–508.
8. Doupnik CA, Davidson N, Lester HA (1995) The inward rectifier potassium channel family. Curr Opin Neurobiol 5: 268–277.
9. Kubo Y, Baldwin TJ, Jan YN, Jan LY (1993) Primary structure and functional expression of a mouse inward rectifier potassium channel. Nature 362: 127–133.
10. Koyama H, Morishige KI, Takahashi N, Zanelli JS, Fass DN, et al. (1994) Molecular cloning, functional expression and localization of a novel inward rectifier potassium channel in the rat brain. FEBS Lett 341: 303–307.
11. Périer F, Radeke CM, Vandenberg CA (1994) Primary structure and characterization of a small-conductance inwardly rectifying potassium channel from human hippocampus. Proc Natl Acad Sci USA 91: 6240–6244.
12. Takahashi N, Morishige KI, Jahangir A, Yamada M, Findlay I, et al. (1994) Molecular cloning and functional expression of cDNA encoding a second class of inward rectifier potassium channels in the mouse brain. J Biol Chem 269: 23274–23279.
13. Töpert C, Döring F, Wischmeyer E, Karschin C, Brockhaus J, et al. (1998) Kir2.4: a novel K^+ inwardly rectifier channel associated with motoneurons of cranial nerve nuclei. J Neurosci 18: 4096–4105.
14. Karschin C, Dißmann E, Stuhmer W, Karschin A (1996) IRK(1-3) and GIRK(1-4) inwardly rectifying K^+ channel mRNAs are differentially expressed in the adult rat brain. J Neurosci 16: 3559–3570.
15. Inanobe A, Fujita A, Ito M, Tomoike H, Inageda K, et al. (2002) Inward rectifier K^+ channel Kir2.3 is localized at the postsynaptic membrane of excitatory synapes. Am J Physiol 282: C1396–1403.
16. Coulter KL, Périer F, Radeke CM, Vandenberg CA (1995) Identification and molecular localization of a pH-sensing domain for the inward rectifier potassium channel HIR. Neuron 15: 1157–1168.
17. Muñoz V, Vaidyanathan R, Tolkacheva EG Dhamoon AS, Taffet SM, et al. (2007) Kir2.3 isoform confers pH sensitivity to heteromeric Kir2.1/Kir2.3 channels in HE293 cells. Heart Rhythm 4: 487–496.
18. Ureche ON, Baltaev R, Ureche L, Strutz-Seebohm N, Lang F, et al. (2008) Novel insights into the structural basis of pH-sensitivity in inward rectifier K^+ channels Kir2.3. Cell Physiol Biochem 21: 347–356.
19. Preisig-Müller R, Schlichthörl G, Goerge T, Heinen S, Brüggemann A, et al. (2002) Heteromerization of Kir2.x potassium channels contributes to the phenotype of Andersen's syndrome. Proc Natl Acad Sci USA 99: 7774–7779.
20. Schram G, Pourrier M, Wang Z, White M, Nattel S (2003) Barium block of Kir2 and human cardiac inward rectifier currents: evidence for subunit-heteromeric contribution to native currents. Cardiovasc Res 59: 328–338.
21. Zhang H, Yan X, Mirshahi T, Logothetis DE (2001) Agonist-induced inhibition of IRK3 is dependent on hydrolysis of PIP_2. Biophys J 80: 629a.
22. Liu Y, Liu D, Heath L, Meyers DM, Krafte DS, et al. (2001) Direct activation of an inwardly rectifying potassium channel by arachidonic acid. Mol Pharmacol 59: 1061–1068.
23. Vallée M, Mayo W, Darnaudéry M, Corpéchot C, Young J, et al. (1997) Neurosteroids: deficient cognitive performance in aged rats depends on low pregnenolone sulfate levels in the hippocampus. Proc Natl Acad Sci USA 94: 14865–14870.
24. Reddy DS, Kulkarni SK (1997) Differential anxiolytic effects of neurosteroids in the mirrored chamber behavior test in mice. Brain Res 752: 61–71.
25. Reddy DS, Kaur G, Kulkarni SK (1998) Sigma (σ_1) receptor mediated antidepressant-like effects of neurosteroids in the Porsolt forced swim test. Neuroreport 14: 3069–3073.
26. Mayo W, Le Moal M, Abrous DN (2001) Pregnenolone sulfate and aging of cognitive functions: behavioral, neurochemical, and morphological investigations. Horm Behav 40: 215–217.
27. Shirakawa H, Katsuki H, Kume T, Kaneko S, Akaike A (2005) Pregnenolone sulphate attenuates AMPA cytotoxicity on rat cortical neurons. Eur J Neurosci 32: 2329–2335.
28. Williamson J, Mtchedlishvili Z, Kapur J (2004) Characterization of the convulsant action of pregnenolone sulfate. Neuropharmacology 46: 856–864.
29. Chen SC, Liu BC, Chen CW, Wu FS (2006) Intradermal pregnenolone sulfate attenuates capsaicin-induced nociception in rats. Biochem Biophys Res Comm 349: 626–633.
30. Reddy DS, Kulkarni SK (1997) Chronic neurosteroid treatment prevents the development of morphine tolerance and attenuates abstinence behavior in mice. Eur J Pharmacol 337: 19–25.
31. Reddy DS, Kulkarni SK (1997) Neurosteroids coadministration prevents development of tolerance and augments recovery from benzodiazepine withdrawal anxiety and hyperactivity in mice. Methods Find Exp Clin Pharmacol 19: 395–405.
32. Wang MD, Wahlström G, Bäckström T (1997) The regional brain distribution of the neurosteroids pregnenolone and pregnenolone sulfate following intravenous infusion. J Steroid Biochem Mol Biol 62: 299–306.
33. Stonehouse AH, Pringle JH, Norman RI, Stanfield PR, Conley EC, et al. (1999) Characterisation of Kir2.0 proteins in the rat cerebellum and hippocampus by polyclonal antibodies. Histochem Cell Biol 112: 457–465.
34. Prüss H, Derst C, Lommel R, Veh RW (2005) Differential distribution of individual subunits of strongly inwardly rectifying potassium channels (Kir2 family) in rat brain. Mol Brain Res 139: 63–79.
35. Cohen NA, Brenman JE, Snyder SH, Bredt DS (1996) Binding of the inwardly rectifier K^+ channel Kir2.3 to PSD-95 is regulated by protein kinase A phosphorylation. Neuron 17: 759–767.
36. Liu Y, Liu D, Printzenhoff D, Coghlan MJ, Harris R, et al. (2002) Tenidap, a novel anti-inflammatory agent, is an opener of the inwardly rectifying K^+ channel hKir2.3. Eur J Pharmacol 435: 153–160.
37. Corpéchot C, Synguelakis M, Talha S, Axelson M, Sjövall J, et al. (1983) Pregnenolone and its sulfate ester in the rat brain. Brain Res 270: 119–125.
38. Kimoto T, Tsurugizawa T, Ohta Y, Makino J, Tamura HO, et al. (2001) Neurosteroid synthesis by cytochrome P450-containing systems localized in the rat brain hippocampal neurons: *N*-methyl-D-aspartate and calcium-dependent synthesis. Endocrinology 142: 3578–3589.
39. Higashi T, Sugitani H, Yagi T, Shimada K (2003) Studies on neurosteroids: XVI. Levels of pregnenolone sulfate in rat brains determined by enzyme-linked immunosorbent assay not requiring solvolysis. Biol Pharm Bull 26: 709–711.
40. Liu S, Sjövall J, Griffiths WJ (2003) Neurosteroids in rat brain: extraction, isolation, and analysis by nanoscale liquid chromatography-electrospray mass spectrometry. Anal Chem 75: 5835–5846.
41. Mameli M, Carta M, Partrige LD, Valenzuela CF (2005) Neurosteroid-induced plasticity of immature synapses via retrograde modulation of presynaptic NMDA receptors. J Neurosci 25: 2285–2294.
42. Barbaccia ML, Roscetti G, Trabucchi M, Mostallino MC, Concas A, et al. (1996) Time-dependent changes in rat brain neuroactive steroid concentrations and $GABA_A$ receptor function after acute stress. Neuroendocrinology 63: 166–172.
43. Torres JM, Ortega E (2003) DHEA, PREG and their sulfate derivatives on plasma and brain after CRH and ACTH administration. Neurochem Res 28: 1187–1191.
44. Nguyen PN, Yan EB, Castillo-Melendez M, Walker DW, Hirst JJ (2004) Increased allopregnanolone levels in the fetal sheep brain following umbilical cord occlusion. J Physiol 560: 593–602.
45. Caldeira JC, Wu Y, Mameli M, Purdy RH, Li PK, et al. (2004) Fetal alcohol exposure alters neurosteroid levels in the developing rat brain. J Neurochem 90: 1530–1539.
46. Yan CZ, Hou YN (2004) Effects of morphine dependence and withdrawal on levels of neurosteroids in rat brain. Acta Pharmacol Sin 25: 1285–1291.
47. Iwamori M, Moser HW, Kishimoto Y (1976) Steroid sulfatase in brain: comparison of sulfohydrolase activities for various steroid sulfates in normal and pathological brains, including the various forms of metachromatic leukodystrophy. J Neurochem 27: 1389–1395.
48. Park IH, Han BK, Jo DH (1997) Distribution and characterization of neurosteroid sulfatase from the bovine brain. J Steroid Biochem Mol Biol 62: 315–320.
49. Steckelbroeck S, Nassen A, Ugele B, Ludwig M, Watzka M, et al. (2004) Steroid sulfatase (STS) expression in the human temporal lobe: enzyme activity, mRNA expression and immunohistochemistry study. J Neurochem 89: 403–417.
50. Mi H, Deerinck TJ, Jones M, Ellisman MH, Schwarz TL (1996) Inwardly rectifying K^+ channels that may participate in K^+ buffering are localized in microvilli of Schwann cells. J Neurosci 16: 2421–2429.
51. Le Maout SL, Brejon M, Olsen O, Merot J, Welling PA (1997) Basolateral membrane targeting of a renal-epithelial inwardly rectifying potassium channel from the cortical collecting duct, CCD-IRK3 in MDCK cells. Proc Natl Acad Sc USA 94: 13329–13334.
52. Melnyk P, Zhang L, Shrier A, Nattel S (2002) Differential distribution of Kir2.1 and Kir2.3 subunits in canine atrium and ventricule. Am J Physiol 283: H1123–1133.
53. Havlíková H, Hill M, Hampl R, Stárka L (2002) Sex- and age-related changes in epitestesterone in relation to pregnenolone sulfate and testosterone in normal subjects. J Clin Endocrinol Metab 87: 2225–2231.
54. de Peretti E, Forest MG, Loras B, Morel Y, David M, et al. (1986) Usefulness of plasma pregnenolone sulfate in testing pituitary-adrenal function in children. Acta Endocrinol Suppl 279: 259–263.
55. Hill M, Parizek A, Klak J, Hampl R, Sulcová J, et al. (2002) Neuroactive steroids, their precursors and polar conjugates during parturition and postpartum in maternal and umbilical blood: 3.3β-hydroxy-5-ene steroids. J Steroid Biochem Mol Biol 82: 241–250.

56. Bicíková M, Tallová J, Hill M, Krausová Z, Hampl R (2000) Serum concentrations of some neuroactive steroids in women suffering from mixed anxiety-depressive disorder. Neurochem Res 25: 1623–1627.
57. Hill M, Popov P, Havlíková H, Kancheva L, Vrbíková J, et al. (2005) Altered profiles of serum neuroactive steroids in premenoposal women treated for alcohol addiction. Steroids 70: 515–524.
58. Tagawa N, Tamanaka J, Fujinami A, Kobayashi Y, Takano T, et al. (2000) Serum dehydroepiandrosterone, dehydroepiandrosterone sulfate and pregnenolone sulfate concentrations in patients with hyperthyroidism and hypothyroidism. Clin Chem 46: 523–528.
59. Morfin R, Young J, Corpéchot C, Egestad B, Sjövall J, et al. (1992) Neurosteroids: pregnenolone in human sciatic nerves. Proc Natl Acad Sci USA 89: 6790–6793.
60. Akwa Y, Schumacher M, Jung-Testas I, Baulieu EE (1993) Neurosteroids in rat sciatic nerves and Schwann cells. C R Acad Sci III 316: 410–414.
61. Kobayashi T, Ikeda K, Ichikawa T, Abe S, Togashi S, et al. (1995) Molecular cloning of a mouse G-protein-activated K^+ channel (mGIRK1) and distinct distributions of three GIRK (GIRK1, 2 and 3) mRNAs in mouse brain. Biochem Biophys Res Commun 208: 1166–1173.
62. Kobayashi T, Ikeda K, Kojima H, Niki H, Yano R, et al. (1999) Ethanol opens G-protein-activated inwardly rectifying K^+ channels. Nat Neurosci 2: 1091–1097.
63. Kobayashi T, Ikeda K, Kumanishi T (2000) Inhibition by various antipsychotic drugs of the G-protein-activated inwardly rectifying K^+ (GIRK) channels expressed in *Xenopus* oocytes. Br J Pharmacol 129: 1716–1722.
64. Ho K, Nichols CG, Lederer WJ, Lytton J, Vassilev PM, et al. (1993) Cloning and expression of an inwardly rectifying ATP-regulated potassium channel. Nature 362: 31–38.
65. Kobayashi T, Ikeda K, Kumanishi T (2002) Functional characterization of an endogenous *Xenopus* oocyte adenosine receptor. Br J Pharmacol 135: 313–322.
66. Ikeda K, Yoshii M, Sora I, Kobayashi T (2003) Opioid receptor coupling to GIRK channels. In vitro studies using a Xenopus oocyte expression system and in vivo studies on weaver mutant mice. Methods Mol Med 84: 53–64.
67. Kobayashi T, Washiyama K, Ikeda K (2003) Inhibition of G protein-activated inwardly rectifying K^+ channels by fluoxetine (Prozac). Br J Pharmacol 138: 1119–1128.

Int. J. Environ. Res. Public Health **2009**, *6*, 2205-2225; doi:10.3390/ijerph6082205

OPEN ACCESS

International Journal of
Environmental Research and Public Health
ISSN 1660-4601
www.mdpi.com/journal/ijerph

Article

Verification of the Addiction Severity Index Japanese Version (ASI-J) as a Treatment-Customization, Prediction, and Comparison Tool for Alcohol-Dependent Individuals

Ayako Haraguchi [1], Yasukazu Ogai [1], Eiichi Senoo [2], Satoru Saito [3], Yoshihiro Suzuki [4], Aihide Yoshino [5], Aro Ino [6], Kenji Yanbe [7], Mitsuru Hasegawa [8], Masaru Murakami [9], Masanobu Murayama [10], Toru Ishikawa [11], Susumu Higuchi [12] and Kazutaka Ikeda [1,*]

1 Division of Psychobiology, Tokyo Institute of Psychiatry, 2-1-8 Kamikitazawa, Setagaya-ku, Tokyo 156-8585, Japan; E-Mails: haragu-a@prit.go.jp (A.H.); y-oogai@prit.go.jp (Y.O.)
2 Division of Social Psychiatry, Tokyo Institute of Psychiatry, 2-1-8 Kamikitazawa, Setagaya-ku, Tokyo 156-8585, Japan; E-Mail: senoo@prit.go.jp
3 Institute for Family Functioning, 2-14-6 Azabu Ju-ban, Minato-ku, Tokyo 106-0045, Japan; E-Mail: yamanaka@iff.or.jp
4 Wakamiya Hospital, 2-15-3 Yoshiwara, Yamagata 990-2451, Japan; E-Mail: wakamiya@koutoku.or.jp
5 National Defense Medical College Hospital, 3-2 Namiki, Tokorozawa, Saitama 359-8513, Japan; E-Mail: aihide@me.ndmc.ac.jp
6 Dansyu no Ie Clinic, 217 Fujikata, Tsu, Mie 514-0815, Japan; E-Mail: aroino@za.ztv.ne.jp
7 Asahiyama Hospital, 4-3-33 Futagoyama, Chuo-ku, Sapporo, Hokkaido 064-0946, Japan; E-Mail: a-ikyoku@gray.plala.or.jp
8 Okabe Hospital, 15 Nagasaka-machi-chi, Kanazawa, Ishikawa 921-8114, Japan; E-Mail: hasegawamitsuru@okabe-net.jp
9 National Hospital Organization Ryukyu Hospital, 7958-1, Kin, Kin-Cho, Kunigami-Gun, Okinawa 904-1201, Japan; E-Mail: murakami@m.email.ne.jp
10 Akagi-Kohgen Hospital, Kitaakagiyama, Akagi-machi, Shibukawa, Gunma 379-1111, Japan; E-Mail: masamura@msa.biglobe.ne.jp
11 Tohokukai Mental Hospital, 1-8-7, Kashiwagi, Aoba-ku, Sendai, Miyagi 981-0933, Japan; E-Mail: tishikawa@tohokukai.com
12 National Hospital Organization Kurihama Alcoholism Center, 5-3-1, Nobi, Yokosuka, Kanagawa 246-0841, Japan; E-Mail: h-susumu@db3.so-net.ne.jp

* Author to whom correspondence should be addressed; E-Mail: ikedak@prit.go.jp;
Tel.: +81-3-3304-5701 ext. 508; fax: +81-3-3329-8035

Received: 7 July 2009 / Accepted: 10 August 2009 / Published: 12 August 2009

Abstract: *Objective:* To demonstrate the usefulness of the Addiction Severity Index Japanese Version (ASI-J) in Japanese alcohol-dependent individuals. The ASI is a frequently used clinical and research instrument that measures severities in seven functional domains in people with substance abuse disorders. *Methods:* A total of 370 male inpatients with a history of alcohol dependence participated in the study. Forty-nine participants were excluded in the final analysis due to lack of reliability (i.e., patient misrepresentation or inability to understand). We used the ASI-J and a series of indexes that determined patient states during and post-treatment. *Results:* The correlations between ASI Composite Scores (CSs), which were calculated through a weighted formula and indicated the severity of each problem area, were significant but low in eight relations and not significant in 13 relations, indicating substantial independence of the problem areas. Significant differences were found in Family/Social CSs between abstinent and relapsed alcohol-dependent individuals. The questions of undesirable attitude were significantly related to the CSs of Employment, Drug use, Family/Social, and Psychiatric sections. Significant differences were observed in patient demographics, CS, and ASI Severity Rating (SR) and interviewer's subjective scoring between alcohol-dependent individuals and drug abusers. CSs in Japanese alcohol-dependent individuals were generally similar to corresponding CSs in individuals from other countries, with the exception of The Netherlands. *Conclusions:* This study demonstrated that the ASI-J is useful for understanding individual profiles of problems for each patient and planning customized treatment. The ASI-J served as a predictive tool for relapse and compliance to treatment afterward and was shown to be useful as a comparison tool in clarifying similarities and differences between substance abuser groups.

Keywords: addiction severity index; alcohol dependence; japanese

1. Introduction

The appearance of alcohol dependence and its related disorders is hypothesized to be attributable to a patient's biological basis combined with psychological and social factors [1,2] such that each patient with alcohol dependence has individually different issues. Addicted patients cannot be adequately characterized simply by measuring the nature, amount, and duration of their substance use [3]. Addiction-related problems are typically reasons for referral to addiction treatment, are often of greater concern to the patient than the substance use itself, and are usually important for deciding the setting and content of care [3]. Therefore, customizing treatment for individual patients according

to their problems and motivation toward treatment is ideal. However, no prevailing methods exist, at least in Japan, to comprehensively reveal multidimensional patient states related to treatment.

In addition to the difficulty in revealing patient states, the outcome of alcohol dependence treatment is difficult to evaluate, partially because predicting patient compliance to treatment and risk of relapse is difficult. Tools predicting a patient's prognosis will enable treatment staff to provide additional and adequate care to the patient.

To clinically apply the results of substance dependence studies, tools for comparing patient groups are useful. For example, when medicine and treatment approaches are used in different patient groups, understanding the similarities and differences of patient features and their treatment environments is critical. The wide use of common tools enables clinicians and researchers to compare patients with different demographics, patients with different substance dependence, patients in different countries, and patients and healthy controls. Such common assessment tools are also useful to grasp the profiles of target patient groups and refine treatment modalities.

The Addiction Severity Index (ASI) [4] is an epochal interview developed to achieve the aforementioned goals. Currently, the ASI has reached its fifth version [5], and the instrument has been translated into over 20 languages [3]. The application of the ASI to alcohol-dependent individuals has been verified in various countries (The Netherlands, Switzerland, United States, Germany [1,5-9]), and the ASI has nearly achieved both reliability and validity, although some problems still exist [10].

The ASI is a semi-structured clinical research interview designed to assess problem severity in seven functional domains: Medical, Employment/Support, Alcohol use, Drug use, Legal, Family/Social relationships, and Psychiatric. The ASI provides two types of overall scores for respective problem areas to rate the severity of the problem [11], including the composite score (CS) and the severity rating (SR). The CS is an objective score calculated through a weighted formula designed to provide an equal contribution from each item. The SR is a relatively subjective score indicating the need for additional treatment in the specific area based on interviewer assessment. The ASI has a system to clearly indicate a change of two severity scores by administering it before and after treatment. The ASI Japanese version (ASI-J) was applied to patients with a history of drug abuse, and its reliability and validity have already been confirmed [12]; however, the ASI-J has not yet been applied to patients with a history of alcohol dependence.

In the present study, we investigated the usefulness of the ASI-J in alcohol-dependent individuals in Japan to determine (*i*) its usefulness as a tool for understanding problem profiles for each patient, (*ii*) its usefulness as a tool to determine patient prognosis, and (*iii*) its usefulness as a common assessment tool for comparison studies.

2. Methods

2.1. Participants

A total of 370 male inpatients with a history of alcohol dependence participated in the study. The participants were recruited from nine nationwide hospitals for addiction treatment in Japan (n = 91, National Hospital Organization Kurihama Alcoholism Center, Kanagawa; n = 55, Wakamiya Hospital, Yamagata; n = 50, Komakino Hospital, Tokyo; n = 42, Mie Prefectural Mental Medical Center, Mie;